Marine Geology 348 (2014) 88–102

Contents lists available at ScienceDirect

Marine Geology

journal homepage: www.elsevier.com/locate/margeo

The Glacial–Interglacial transition and Holocene environmental changes in sediments from the Gulf of Taranto, central Mediterranean

Marie-Louise S. Goudeau [a,*,1], Anna-Lena Grauel [b,**,1], Chiara Tessarolo [c], Arne Leider [d,e], Liang Chen [e], Stefano M. Bernasconi [b], Gerard J.M. Versteegh [d,e], Karin A.F. Zonneveld [d,e], W. Boer [f], C.M. Alonso-Hernandez [g], Gert J. De Lange [a]

[a] Dept. of Earth Sciences, Geochemistry, Utrecht University, 3508 Utrecht, The Netherlands
[b] Geological Institute, ETH Zurich, 8092 Zurich, Switzerland
[c] Milan-Bicocca University, 20123 Milan, Italy
[d] MARUM Center for Marine Environmental Science, 28334 Bremen, Germany
[e] Dept. of Geoscience, University of Bremen, 28334 Bremen, Germany
[f] Royal NIOZ, Texel, The Netherlands
[g] Centro de Estudios Ambientales de Cienfuegos, Cuba

ARTICLE INFO

Article history:
Received 5 September 2012
Received in revised form 26 November 2013
Accepted 5 December 2013
Available online 12 December 2013

Communicated by J.T. Wells

Keywords:
Holocene climate variability
hydrological changes
NAO
high-resolution records
XRF scans
central Mediterranean Sea

ABSTRACT

An extensive, high-resolution, sedimentological–geochemical survey was done using geo-acoustics, XRF-core scans, ICP-AES, AMS ^{14}C-dating and grain size analyses of sediments in 11 cores from the Gulf of Taranto, the southern Adriatic Sea, and the central Ionian Sea spanning the last 16 cal. ka BP. Comparable results were obtained for cores from the Gallipoli Shelf (eastern Gulf of Taranto), and the southern Adriatic Sea suggesting that the dominant provenance of Gallipoli Shelf sediments is from the western Adriatic mud belt. The ^{210}Pb and ^{14}C-dated high-accumulation-rate sediments permit a detailed reconstruction of climate variability over the last 16 cal. ka BP. Although, the Glacial–Interglacial transition is generally dry and stable these conditions are interrupted by two phases of increased detrital input during the Bølling–Allerød and the late Younger Dryas. The event during the Younger Dryas period is characterized by increased sediment inputs from southern Italian sources. This suggests that run-off was higher in southern- compared to northern Italy. At approximately ~7 cal. ka BP, increased detrital input from the Adriatic mud belt, related to sea level rise and the onset of deep water formation in the Adriatic Sea, is observed and is coincident with the end of sapropel S1 formation in the southern Adriatic Sea. During the mid-to-late Holocene we observed millennial-scale events of increased detrital input, e.g. during the Roman Humid Period, and of decreased detrital input, e.g., Medieval Warm Period. These dry/wet spells are consistent with variability in the North Atlantic Oscillation (NAO). A negative state of the NAO and thus a more advanced penetration of the westerlies into the central Mediterranean, that result in wet conditions in the research area concord with events of high detrital input e.g., during the Roman Humid Period. In contrast, a positive state of the NAO, resulting in dry conditions in the Mediterranean, dominated during events of rapid climate change such as the Medieval Warm Period and the Bronze Age.

1. Introduction

During the Holocene, millennial-scale climatic events such as the 'Medieval Warm Period' (MWP) and the 'Little Ice Age' (LIA) can be detected across the Northern Hemisphere (NH), and have been associated with changes in atmospheric circulation and solar variability (deMenocal et al., 2000; Bond et al., 2001; Rohling et al., 2002; Mayewski et al., 2004). These events have site-specific expressions, and their controlling factors and natural feedback mechanisms are still not fully understood (Mayewski et al., 2004). Therefore, full comprehension of this millennial-scale climatic variability requires long, continuous, high-resolution records from climate-sensitive areas. The Mediterranean region is situated between the subtropical high-pressure belt and the mid-latitude westerlies, recording both high- and low-latitude climate changes, such as those related to the North Atlantic Oscillation (NAO), El Niño Southern Oscillation (ENSO), and Asian Monsoon (Rossignol-Strick, 1985; Hurrell, 1995; Alpert et al., 2006; Lionello et al., 2006; Trigo et al., 2006; Brandimarte et al., 2011; Nieto-Moreno et al., 2011).

Orbital-scale climate changes are reflected by organic-rich sapropel layers in Mediterranean sediment that have been related

* Corresponding author. Tel.: +31 30 253 4991; fax: +31 30 253 5302.
** Correspondence to: A.-L. Grauel, Department of Earth Sciences, University of Cambridge, Cambridge, UK.
E-mail addresses: m.s.goudeau@uu.nl (M.-L.S. Goudeau), alg62@cam.ac.uk (A.-L. Grauel).
[1] Authors contributed equally to this work.

0025-3227/$ – see front matter © 2013 Elsevier B.V. All rights reserved.
http://dx.doi.org/10.1016/j.margeo.2013.12.003

with predominately low-latitude forcing (Rossignol-Strick, 1985; Hilgen, 1991; Lourens et al., 1996; De Lange et al., 2008). High-latitude climate variability has been associated to millennial to decadal changes in dust transport, temperature, precipitation, and deep-water formation in the Mediterranean region (e.g., Cini Castagnoli et al., 1999; Schilman et al., 2001; Rohling et al., 2002; Sangiorgi et al., 2003; Frisia et al., 2005; Piva et al., 2008; Gennari et al., 2009; Jilbert et al., 2010a, 2010b). Climate reconstructions of the Adriatic Sea region suggest that cold events coincide with North Atlantic ice-rafting events (Sangiorgi et al., 2003; Piva et al., 2008). In addition, late Holocene records in particular from the Adriatic area suggest that it was generally wetter and warmer during the 'Roman Humid Period' (RHP), drier and warmer during the MWP, but relatively cold and wet during the LIA (e.g., Sangiorgi et al., 2003; Frisia et al., 2005; Piva et al., 2008; Chen et al., 2011, 2013; Giraudi et al., 2011; Grauel et al., 2013b). Cold and warm spells are thought to affect Adriatic Deep Water (ADW) formation and consequently the general Mediterranean ocean circulation (Sangiorgi et al., 2003; Piva et al., 2008). Late Holocene records in lakes reveal contrasting millennial scale hydrological patterns between northern Italy (>43°N) and southern Italy (<43°N; e.g., Magny et al., 2003; Joannin et al., 2012). This suggests shifts in the extent of the westerlies (i.e. NAO) and indicates that these events are characterized by complex patterns and expressions.

Climate records based on marine sediments from the southern Adriatic and the central Mediterranean Sea that cover the entire Holocene and deglaciation are rare and mostly focus on Sea Surface Temperature (SST) reconstructions based on faunal assemblages or oxygen isotopes (e.g., Rohling et al., 2002; Sangiorgi et al., 2003; Piva et al, 2008). Sub-decadal to centennial scale variability has been observed in the Gallipoli Shelf sediments for carbonate contents (Cini Castagnoli et al., 1992), stable oxygen isotopes of *Globigerinoides ruber* (e.g., Cini Castagnoli et al., 1999; Grauel et al., 2013a, 2013b), $U^{k}{}_{37'}$ (Versteegh et al., 2007; Grauel et al., 2013a) and dinoflagellate cysts (Chen et al., 2011, 2013; Zonneveld et al., 2012). This variability has been related to changes in SST, salinity and eutrophication caused by changes in river discharge, the NAO, and solar variability. Only a few limited studies have been reported on recent sediment transport and geochemical patterns in the Gulf of Taranto indicating a complex and spatially different morphology, sedimentation, and chemical composition as well as a connection with the Adriatic Sea (Rossi et al., 1983; Buccolieri et al., 2006; Malinverno et al., 2010; Goudeau et al., 2013). Surface sediments from the Gulf of Taranto and Southern Adriatic suggest that the geochemical signature of sediments can be used to detect changes in grain size, productivity, and to distinguish a northern from a more southern Italian provenance (Goudeau et al., 2013).

Despite the high potential of this area to reconstruct high-frequency Holocene paleoclimate variability and possible contrasting north/south hydrological patterns, to date no comprehensive studies covering more than 5500 years exist for the Gallipoli Shelf sediments (Cini Castagnoli et al., 1992). This highlights the need for a basin-wide sedimentological study in the Gulf of Taranto to better understand paleoclimatic records from this region. Therefore, we first assess at high resolution the compositional variability, potential correlations and provenance for sediments of all cores of this study area. Subsequently, we focus on sediments from the Gallipoli Shelf, eastern Gulf of Taranto, which are thought to be related to more general, supra-regional climate variability. For sediments of the two most comprehensive and consistent cores, we give an in-depth paleoclimate reconstruction with emphasis on some important Holocene climate phases.

2. Regional setting

2.1. Oceanography

The Gulf of Taranto is situated in the north western Ionian Sea between Calabria and Apulia (Fig. 1). It can be divided into three distinct geological provinces, the Apulian Slope, the Taranto Valley and the eastern Calabrian Margin (Rossi et al., 1983). The main influence on transport along the southern Italian coast is the intensity of the Western Adriatic Current (WAC) which flows in a narrow coastal band from the northern Adriatic Sea into the Gulf of Taranto (Poulain, 2001; Bignami et al., 2007; Turchetto et al., 2007). The WAC has a significant inter-annual variability and its influence along the southern Italian coast and the Gulf of Taranto is higher in winter than in summer (Milligan and Cattaneo, 2007). In the Gulf of Taranto, the less saline waters from the WAC mix with the saline Ionian Surface Water (ISW) from the central Ionian Sea.

The bottom layer of the water column in the southern Adriatic region is characterized by the Adriatic Deep Water (ADW) which is a dense water mass formed by two different processes (Turchetto et al., 2007): 1) during winter NE Bora wind events result in the formation of northern Adriatic dense Deep Water (NAdDW) in the northern Adriatic Sea and 2) deep convection during late winter/early spring results in the formation of Southern Adriatic dense Deep Water (SAdDW) in the southern Adriatic Sea (Artegiani et al., 1997; Vilibić and Orlić, 2002). The NAdDW has an enhanced current and particle flux southwards (Turchetto et al., 2007). Around the Cape Santa Maria di Leuca the bottom currents are more intense than the surface currents and have a strong influence on the sedimentation (Savini and Corselli, 2010).

2.2. Sediment accumulation and provenance

Primary sediment supply into the northern Adriatic Sea comes from the Po River in the North and additional contributions from smaller Alpine and Apennine rivers (Turchetto et al., 2007). The mud wedge (also called Adriatic mud belt) formed by these sediments along the Italian shelf reaches up to 30 m thickness in the North and represents the modern high-stand system from ~5.5 ka BP onwards after early Holocene sea-level rise (Cattaneo et al., 2003; Vigliotti et al., 2008). Sediments can be transported by the WAC to the Gulf of Manfredonia (Weltje and Brommer, 2011), and as far south as the eastern Gulf of Taranto (Goudeau et al., 2013). Sediments from the western Gulf of Taranto have a more local provenance (Goudeau et al., 2013).

3. Material and methods

All cores of this study, except core DP20PC, DP23PC and DP39PC, are from the Apulian Margin, a wide continental shelf with a slight depth gradient towards the deep Taranto Valley (Rossi et al., 1983). The slope is locally affected by slumping and active erosion processes (Rossi et al., 1983), thus pre-site survey Multibeam studies are essential. The bathymetric data are based on the integration of several Multibeam surveys which have been conducted during the *RV Pelagia* cruises DOPPIO (2008) and MACCHIATO (2009). The bathymetric data of the Gulf of Taranto area (grid size 15 m) and for the shallower Adriatic Sea (grid size 10 m) were combined with the GEBCO global grid data (grid size 100 m) and integrated to construct a detailed bathymetric map (Fig. 1).

The gravity cores GeoB10701-5, -10703-5, -10704-5, -10706-4, -10709-6 and -10745-3 have been collected during the *RV Poseidon* cruise "CAPPUCCINO" in June 2006 (Zonneveld et al., 2008; Fig. 1). The piston cores DP30PC, DP23PC and DP20PC have been collected during the *RV Pelagia* cruise "DOPPIO" in October/November 2008, and the piston core MP49PC has been collected during *RV Pelagia* cruise "MACCHIATO" in November/December 2009 De Lange a.c.p., 2009; Fig. 1; Table 1). In the following, these cores will be addressed by their station name only.

3.1. Grain size analyses

The grain size distributions were determined for 5 core top samples (0–2 cm) of multicores GeoB10701, -10703, -10704, -10706, and

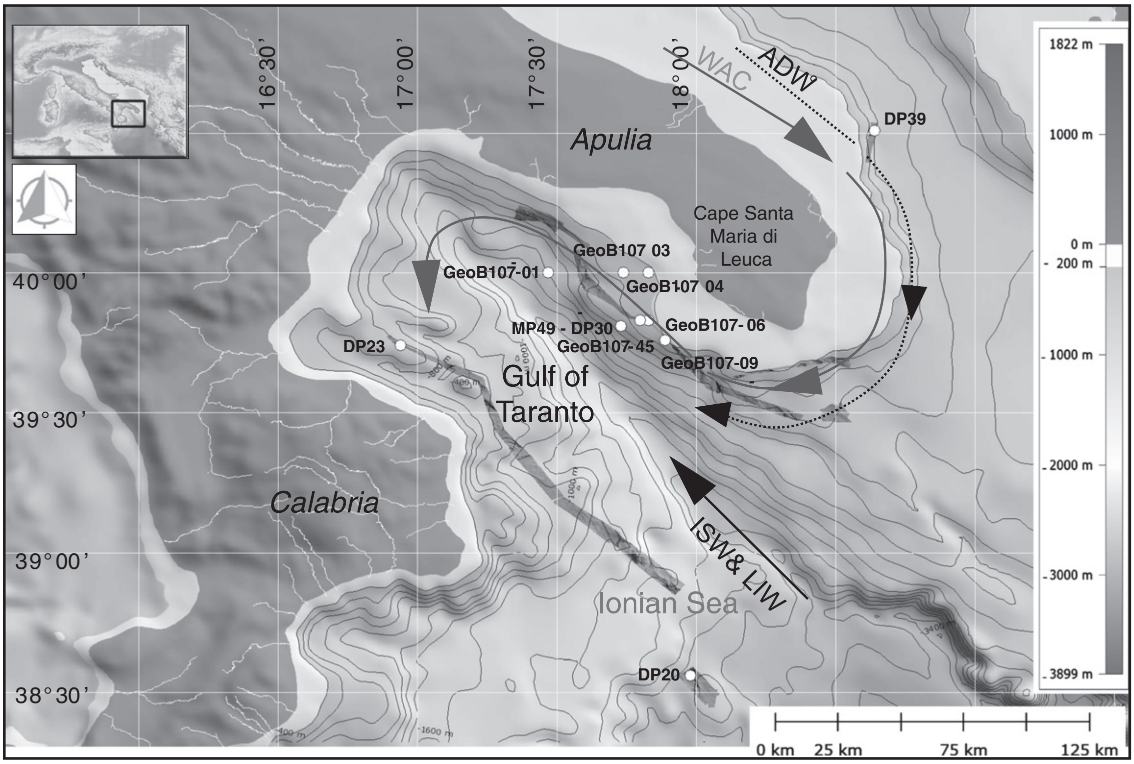

Fig. 1. Bathymetric map of the Gulf of Taranto area; core locations are indicated as well as the general circulation pattern (WAC—Western Adriatic Current, ADW—Adriatic Deep Water, ISW—Ionian Surface Water, LIW—Levantine Intermediate Water).

-10709 using a Malvern Laser Diffraction Grainsizer 2000 with the dispersing module Hydro 2000S (Table 2). For a better disaggregation of the sediment, the samples were suspended in $Na(PO_4)n$ (5 g/l) overnight before measurements.

3.2. AMS ^{14}C-dating

For dating purposes ^{210}Pb was determined for core NU04MC and for the top part of DP30 at the laboratories of CEAC, Cuba and NIOZ, The Netherlands (Fig. 2a & Table 1). In addition, nine samples of core DP30 were picked for planktonic foraminifera and analyzed with a miniaturized radiocarbon dating system (MICADAS) (Ruff et al., 2007; Synal et al., 2007) at the AMS Radiocarbon Dating Laboratory at ETH Zurich (Table 3). Five samples were measured as solid graphite targets and four samples were measured directly as CO_2, where MICADAS was equipped with a gas ion source. The ^{14}C-ages were calibrated with the program OxCal v3.10 (Bronk Ramsey et al., 2009) with the references using the Marine04 calibration curve (Hughen et al., 2004) in combination with the region reservoir correction of 121 $\pm$ 60 (ΔR) in addition to the standard reservoir correction of about 400 yr.

The age models for the other cores in the Gulf of Taranto were determined by correlation to core DP30 using the Ca/Ti curves (see Section 4.3 Correlation of cores) and the program AnalySeries 2.0 by Paillard et al. (1996).

3.3. ICP-AES

The topmost sections of DP30 (0–2.78 m) were sampled at 2.5 mm resolution. The major and minor elemental compositions of the freeze-dried samples were analyzed at 1 cm resolution i.e. every 4th sample, using Inductively Coupled Plasma-Atomic Emission Spectroscopy (ICP-AES) with a Perkin Optima 3000 at Utrecht University. For this purpose 125 mg of sample was dissolved in a mixture of 2.5 ml HF (40%) and 2.5 ml pre-mixed acid (HNO_3 16.25% and $HClO_4$ 45.5%) and heated at 90 °C in a closed reaction vessel for at least 8 h (Reitz and De Lange, 2006). Thereafter, they were dried by evaporating at 160 °C until a gel formed. The gels were then dissolved in 25 ml 1M HNO_3. The relative precision (better than 5%) and accuracy were established by duplicates and in-house standards (ISE-921).

Table 1
Geographic and bathymetric information of the core stations.

Cruise	Station	Latitude	Longitude	Bottom depth (m)	Gravity core length (m)	Used methods
CAPPUCCINO	GeoB10701	40°00 N	17°47 E	1181	2.81	XRF, line scan, multicore grain size
CAPPUCCINO	GeoB10703	40°00 N	17°74 E	277	3.78	XRF, line scan, multicore grain size
CAPPUCCINO	GeoB10704	40°00 N	17°83 E	219	5.52	XRF, line scan, multicore grain size
CAPPUCCINO	GeoB10706	39°83 N	17°83 E	218	4.87	XRF, line scan, multicore grain size
CAPPUCCINO	GeoB10709	39°76 N	17°89 E	172	5.19	XRF, line scan, multicore grain size
CAPPUCCINO	GeoB10745	39°81 N	17°73 E	689	3.99	XRF, line scan
DOPPIO	DP20	38°56 N	17°98 E	2446	5.56	XRF, line scan
DOPPIO	DP23	39°74 N	16°94 E	378	9.06	XRF, line scan
DOPPIO	DP30	39°83 N	17°80 E	270	8.28	XRF, line scan, AMS ^{14}C dating, ICP-AES
DOPPIO	DP39	40°51 N	18°64 E	527	7.96	XRF, line scan
MACCHIATO	MP49	39°83 N	17°80 E	267	9.61	XRF, line scan

Table 2
Grain size distribution of surface sediments taken in the Gulf of Taranto. Columns e–f–g are sub-divisions of the silt fraction (column c), whereas columns h and i represent most of the sand fraction.

A Station	B Clay 0.01–2 μm	C Silt 2–63 μm	D Sand 63–2000 μm	e Fine silt 2–8 μm	f Medium Silt 8–16 μm	g Coarse silt 16–63 μm	h Very fine sand 63–125 μm	i Fine sand 125–250 μm
GeoB10701	20.7	72.8	6.5	36.5	15.1	21.3	5.8	0.6
GeoB10703	20.9	78.3	0.9	44.8	20.7	12.8	0.9	0.0
GeoB10704	17.9	76.5	5.6	36.6	17.0	22.9	5.1	0.5
GeoB10706	18.3	77.5	4.3	40.5	18.7	18.4	3.5	0.6
GeoB10709	19.6	75.0	5.5	38.3	15.7	20.9	4.9	0.5

3.4. Color scanning and XRF analyses

To identify changes in color, the sediments of core DP30 were scanned with a Minolata Colorscan Spectrophotometer CM-508i. Measurements were taken in a 1 cm resolution immediately after opening of the core.

For this study two different XRF core scanners, the AVAATECH core scanner (Richter et al., 2006) and the ITRAX XRF core scanner (COX Analytical Systems), were used (Croudace et al., 2006). The split core halves from the GeoB cores (10704, 10745, 10706, 10703, 10709) were scanned at 2 mm resolution with the ITRAX scanner at the Geography Institute (GEOPOLAR group), University of Bremen. The elements: Si, K, Ca, Ti, V, Cr, Mn, Fe, Rb, Sr, Zr, Br, Pb were measured using a Mo X-ray tube at 30 kV. The cores GeoB10704 and GeoB10709 were additionally measured using a Cr X-ray tube at 30 kV so as to include the lower atomic number elements; the measured elements were: Al, Si, S, K, Ca, Ti and Ba. The count time for each measurement was 30 s. Afterwards, five measurements were averaged so as to have the same 1-cm resolution as used for the cores measured with the AVAATECH core scanner.

The archive halves of the MP and DP cores (MP49, DP30, DP39, DP20, DP23) were scanned at 1 cm resolution with the AVAATECH scanner at the NIOZ in December 2008 (DP-cores: 20, 23, 30, 39) and January 2010 (MP-core: 49). The elements: Al, Si, P, S, Cl, K, Ca, Ti, Cr, Fe, Mn, Co, Rh, were measured at an X-ray voltage of 10 kV, while the elements: Zn, Ga, Br, Rb, Sr, Y, Zr, Au, Pb, Bi and the elements: Sr, Zr, Nb, Mo, Ag, Sn, Te, I, Ba were measured with an X-ray voltage of 30 kV and of 50 kV, respectively. The count time of each measurement was 30 s. In September 2009 the detector in the core scanner was changed which resulted in higher counts in 2010 compared to 2008. In-house standards (SARM4, JB1 and JR1) measured daily during scanning indicate a standard deviation of less than 3% of the average for all elements presented in this study. All results are reported in counts per second.

As XRF core scanning data is considered to be semi-quantitative (Croudace et al., 2006; Richter et al., 2006; Weltje and Tjallingii, 2008), elemental ratios have been used rather than direct counts. The elements Al and Ti are amongst the most commonly used denominators (e.g., Croudace et al., 2006). Both elements are highly correlated and have a similar distribution, best illustrated by the quantitative ICP-AES data (Fig. 3a, b), concurring with results from other studies (e.g., Weltje and Tjallingii, 2008). Consequently, both of them would be suitable as a denominator, but preferably the one with the best reproducibility in XRF-scan data. Ti and Al counts from the XRF core scan indicate a positive trend but poor correlation (Fig. 3a). This is thought to be related to absorption due to water which is more severe for light elements such as aluminum than for more heavy elements such

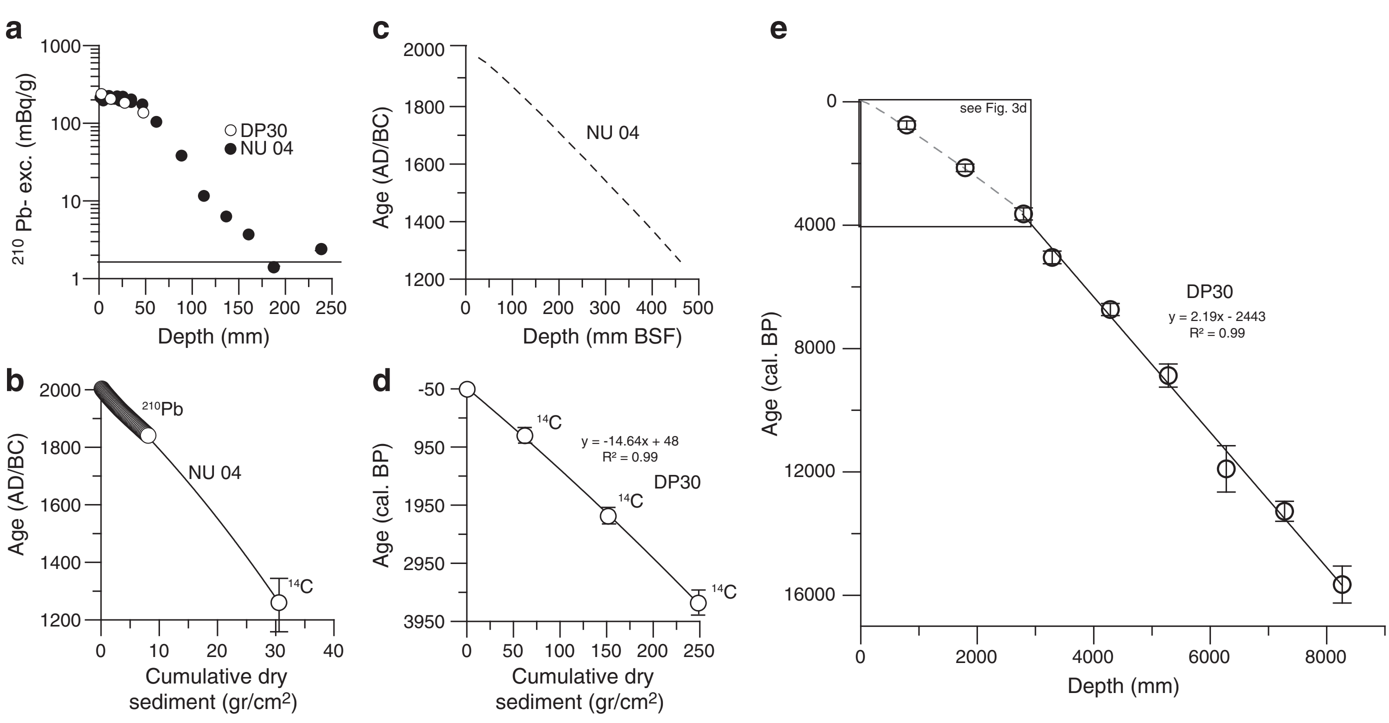

Fig. 2. (a) ^{210}Pb depth profile of NU-04 (black circles) and DP-30 (white circles). Black line indicates the background values for the ^{210}Pb model (b) age model of NU-04 using the cumulative dry sediment and the dating points from the ^{210}Pb-model and radio-carbon dating (c) modeled age versus depth for NU-04 (d) age model of the first 2.5 m of DP30 using the cumulative dry sediment and the dating points from the ^{210}Pb-model and radio-carbon dating (e) entire age model of DP30, the ^{14}C-ages were calibrated with the program OxCal v3.10 (Bronk Ramsey et al., 2009), with atmospheric calibration curve from Reimer et al. (2004) and the marine calibration curve Marine04 from Hughen et al. (2004) ($\Delta R = 121 \pm 60$ years).

as titanium (Tjallingii et al., 2007; Hennekam and De Lange, 2012). Therefore, we will use Ti as a denominator in elemental ratios of XRF scan data. Furthermore, we will only compare trends, not absolute values of the elemental ratios, as small matrix effects may significantly influence instrumental performance within and between XRF-core scanners (Richter et al., 2006; Tjallingii et al., 2007).

4. Results

4.1. Core descriptions and grain size analyses

The sediments from the Gulf of Taranto area and the Adriatic Sea are rather similar in color, grain size and texture whereas deviating observations have been made for sediments from the western Ionian Sea (core DP20: heterogeneous sediments with large variations in color, lamination and erosive horizons). The rather homogeneous sediments across the whole eastern Gallipoli Shelf consist of light gray–brown silty clays with isolated black, organic carbon-rich spots (for complete core descriptions contact authors and see Zonneveld et al. (2008)). In the cores GeoB10703, GeoB10704, and GeoB10745, no distinctive sedimentological features were visible. In the lowermost meter of DP30 and MP49 shell fragments are present and the sediment is coarser. Moreover, the amount of organic carbon-rich spots is enhanced at the bottom of core MP49. In core GeoB10709 the interval 3.9–1.8 m contains much coarser material than below and above it. This core is located relatively close to the shelf edge, in an area potentially influenced by slump events (A. Savini, personal commun.), and is thus possibly affected by slumping and/or erosion (Fig. 1). Therefore, the sediments of this interval are attributed to a slump, and will not be discussed any further.

The grain size distribution for core-top sediments (0–2 cm) in the eastern part of the Gulf of Taranto is slightly bimodal, with elevated percentages in grain size in 2–8 μm (fine silt) and 30–40 μm (coarse silt) size fraction for all cores except GeoB10703 and GeoB10706 (Table 2). The latter lack the elevated percentages in the coarse silt fraction and are uni-modal (Table 2).

4.2. Age model of core DP30

The standard deviation for ^{14}C data in the four samples measured as CO_2 is slightly larger than that for the five samples measured as graphite (Fig. 2b, d, e, Table 3) because of the smaller amount of sample available (~200 μg). Using a model (Boer et al., 2006) with a background of 15 Bq/kg, a sedimentation rate of 0.85 mm/yr with a bioturbation layer of 4.4 cm was determined on the basis of ^{210}Pb data for the upper part of the nearby NU-04 multicore (Fig. 2a, see Grauel et al., 2013a for more detailed description). This model for the upper-most part of the sediment was combined with a ^{14}C date and compared to the cumulative sediment accumulation taking the effects of increasing water content in the upper part into account (Fig. 2b, c). A 1st order polynomial was used to combine ^{210}Pb and ^{14}C ages. During the recovery of DP30, the upper few mm were lost. Comparison between the ^{210}Pb profile of DP30 and NU-04 revealed that this was equivalent to a loss of ~10 years (Fig. 2a). For the age model of DP30 we assumed a linear relationship between cumulative sediment accumulation and ^{14}C dates for the first 2500 mm (Fig. 2d). From this point (2500 mm) onwards, water content and thus compaction is thought to remain stable. Therefore, a linear relationship is assumed between ^{14}C dates and depth (mm) in this part of the core (Fig. 2e). The calibrated age for the bottom of core DP30 at 8270 mm is 15,650 ± 600 cal. yr BP (±95% confidence) and thus includes the Older Dryas (Fig. 2e, Table 3). The latter suggest that the average sedimentation rate in DP30 is around 0.52 mm/yr.

4.3. Correlation of cores

The Ca/Ti ratio provides a distinct and consistent down-core pattern. This is not only related to the relatively good analytical reliability for

Table 3
Age model and calculated sedimentation rates. The ^{14}C-ages were calibrated with the program OxCal v3.10 (Bronk Ramsey et al., 2009), with the atmospheric calibration curve from Reimer et al. (2004) and the marine calibration curve Marine04 from Hughen et al. (2004) (additional reservoir age: $\Delta R = 121 \pm 60$ years).

ETH no	Depth (mm)	Radiocarbon age (^{14}C age BP)	Calibrated age (cal. yr BP)	Error (95%; ±yr)	Comment
38704	789	1290 ± 25	755	135	Graphite target
38703	1792	2535 ± 30	2140	120	Graphite target
40266	2794	3830 ± 40	3635	195	Graphite target
37085	3286	4880 ± 40	5045	205	Graphite target
37086	4285	6395 ± 45	6735	195	Graphite target
42544	5280	8425 ± 118	8875	375	Gas sample
42545	6276	10739 ± 191	11900	750	Gas sample
42542	7276	11922 ± 147	13275	325	Gas sample
42543	8266	13716 ± 171	15650	600	Gas sample

these two elements using XRF core scanning (see also Tjallingii et al., 2007; Hennekam and De Lange, 2012), but also to the different provenances (from predominantly marine to terrestrial) represented by these elements (see Section 5.2). High-resolution ICP-AES data are available for the top 2.8 m of core DP30 (Fig. 3b, c and d). The Ca/Ti data for the two methods have a similar trend and show a high positive correlation (slope = 0.86, $R^2 = 0.76$, $p < 0.01$; Fig. 2d). However, some smaller scale oscillations in the Ca/Ti ratio which cannot be recognized in the XRF scan data are observed in the ICP-AES analyses (Fig. 3c).

Therefore, this ratio was used to correlate all cores to the dated core DP30. Based on a few tie-points, age models of all other cores are reconstructed (Fig. 4 and Supplementary material). All cores from the Gallipoli Shelf show a similar pattern in the upper part but with different sedimentation rates. Below 6.6 m, variations in the Ca/Ti ratio are small and thus correlation is more ambiguous (see Supplementary material). Core GeoB10701 has a very different Ca/Ti profile and could not be correlated to the other cores (Supplementary material).

Sedimentation rates generally decrease with depth in each core, although not to the same extent in all cores (see Supplementary material). No systematic difference in sedimentation rates is observed between the two different coring systems used (see Supplementary material).

No correspondence is observed between Ionian Sea sediments (DP20) and sediments from the eastern Gulf of Taranto as observed in DP30 (Fig. 5). A clear correspondence is found between DP30 and DP39 (southern Adriatic Sea) from 4000 mm onwards, while DP23 (western Gulf of Taranto) resembles DP30 from 1500 mm onwards (Fig. 5).

4.4. Element distributions in cores DP30 and GeoB10704

To study the overall changes in geochemical composition for sediments from the Gallipoli Shelf over the last 15,000 years, Ca/Ti, Fe/Ti, K/Ti, Zr/Ti, Si/Ti, Ba/Ti, Br/Ti and Sr/Ca ratios derived by XRF core scanning are compared for cores DP30 and GeoB10704 (Fig. 6). These two cores have been selected as DP30 is well dated and GeoB10704 is located higher on the shelf at shallower water depth but from the same region and with a similar pattern in sedimentation rate and Ca/Ti ratio (Fig. 6a). Ba/Ti values are lacking for most of GeoB10704, as during these intervals the abundance of barium is below the detection limit for the equipment and setting used for XRF core-scanning of the GeoB cores (Fig. 6f).

During the Glacial–Interglacial transition (16–15 ka BP) Zr/Ti and Ba/Ti values decrease, while Si/Ti increases (Fig. 6d, e and f). The other elements (Ca/Ti, Fe/Ti, K/Ti and Br/Ti) show a relatively stable pattern in both cores (Fig. 6a, b, c and g) from 16 to 10.8 cal. ka BP. A small interruption is found around 12 cal. ka BP when low values of Ca/Ti and Si/Ti and high values of Ba/Ti and Fe/Ti are observed (Fig. 6a, b, e, f).

Sr/Ca values in both cores start to increase from 13 cal. ka BP (GeoB10704) and 11.5 cal. ka BP (DP30), respectively (Fig. 6h). Between

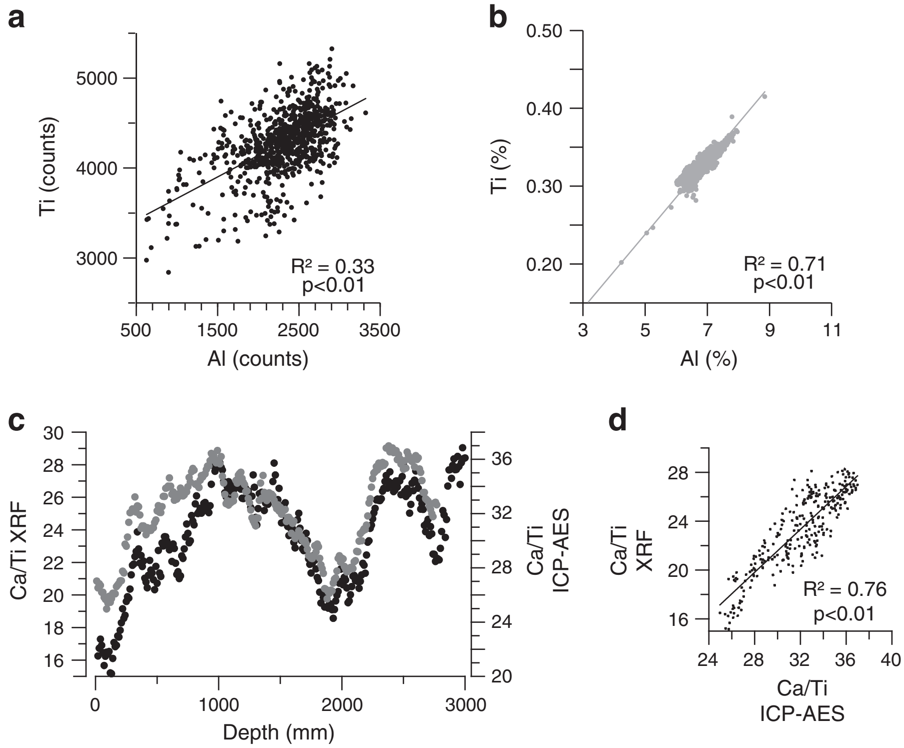

Fig. 3. Correlation between Ti and Al from XRF core scanning (a) and ICP-AES (b). (c) Comparison between Ca/Ti ratio by XRF core scanning (black dots) and by ICP-AES (gray) of the upper ~3 m of core DP30. (d) Correlation between the Ca/Ti ratios as found by both methods.

~11 and 7.5 cal. ka BP Br/Ti values are high in GeoB10704, while they are elevated from 9 to 7.5 cal. ka BP onwards in DP30 (Fig. 6g), which concords with the occurrence of black spots and thus a darker color of the sediments (Fig. 6i). Both cores show a step-wise increase in Fe/Ti around 9 cal. ka BP (Fig. 6b). This increase is coherent with a peak of K/Ti (Fig. 6c) and Zr/Ti (Fig. 6d) and relatively low Ca/Ti values (Fig. 6a) in both cores (~8.7 cal. ka BP). The highest Ca/Ti values are found around 8.3 cal. ka BP. From ~8.3 to 0.5 cal. ka BP Ca/Ti, K/Ti, Zr/Ti, Si/Ti and Ba/Ti show a decreasing trend, while the Fe/Ti ratio increases (Fig. 6).

On top of these general trends, millennial-scale oscillations are observed for the Ca/Ti and Si/Ti ratios (Fig. 6a, e), and to some extent in the Fe/Ti, K/Ti, Zr/Ti (GeoB10704), Ba/Ti (DP30) and Sr/Ca ratios (GeoB10704; Fig. 6b, c, d, f, h).

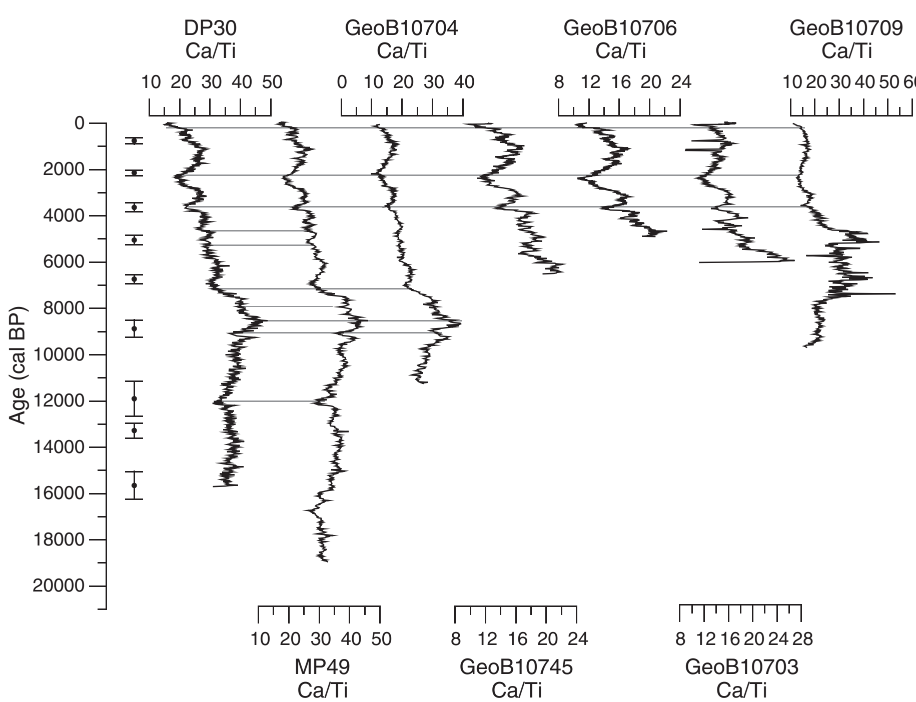

Fig. 4. Age models of the cores from the Gallipoli Shelf calculated from the ^{14}C-dated DP30 core (black dots with corresponding error bars) by correlation of the Ca/Ti curves (see Supplementary Material), and using the program AnalySeries 2.0, by D. Paillard et al. (1996). The continuous lines mark the calibration tie points.

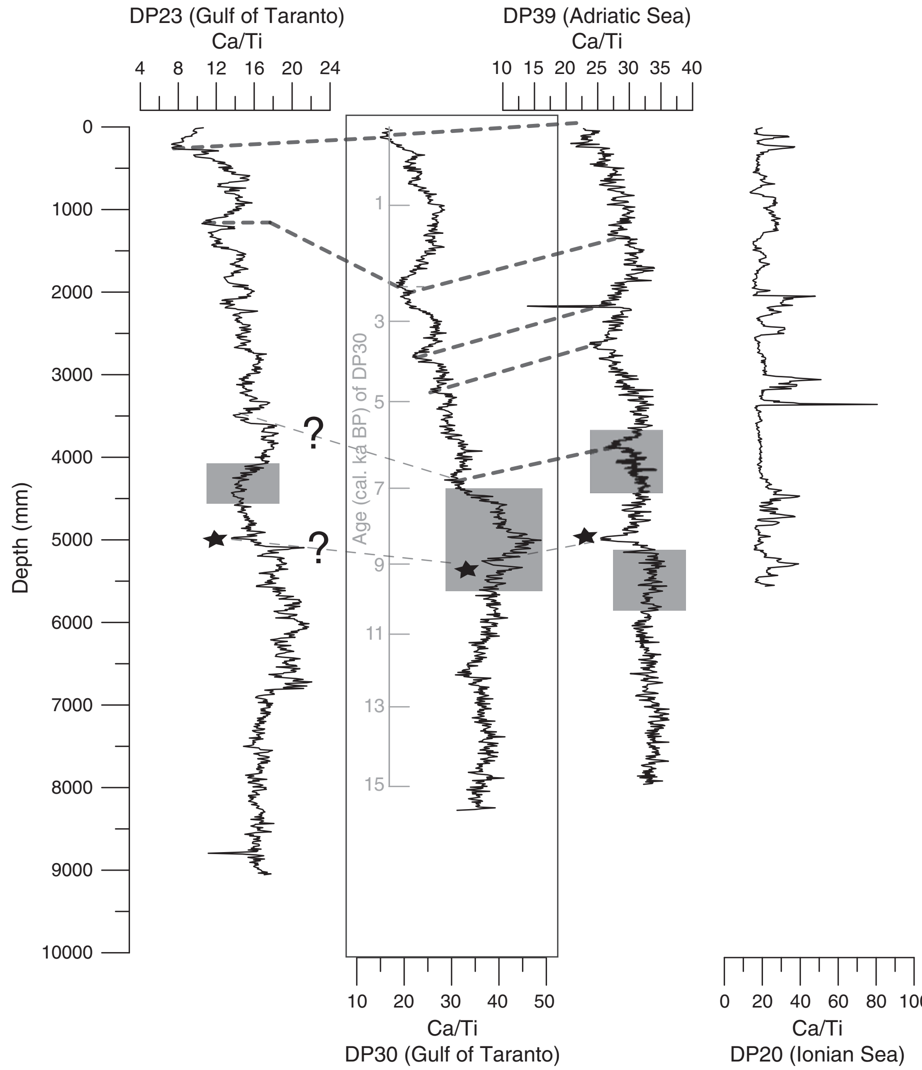

Fig. 5. Ca/Ti ratios of the cores DP23 (western part of the Gulf of Taranto), DP30 (eastern part of the Gulf of Taranto), DP39 (Adriatic Sea), and DP20 (Ionian Sea). Note that all Ca/Ti values are plotted against depth (mm) and that the gray vertical axes represent the age (cal. ka BP) of core DP30. The dashed lines indicate possible correlations. Gray boxes indicate intervals with more black particles, most likely corresponding to sapropel S1 formation. Stars indicate the possible tephra layer of the Mercato eruption.

5. Discussion

Potential variations in the detrital input will not only affect the terrestrial solid-phase fluxes but indirectly – via variations in dissolved riverine nutrient fluxes – also the marine primary productivity related fluxes. The terrigenous solid-phase fluxes can potentially originate from re-sedimentation of shelf sediments, and from input by local and by more remote (Adriatic) riverine systems, all of which are influenced by prevailing current directions and strengths (see Section 2: Regional setting). In addition, a minor eolian (Saharan) contribution is possible: for the present day, 2/3 of the terrigenous fluxes to the central Ionian Sea sediments have been reported to result from eolian dust (e.g., Correggiari et al., 1989; Rutten et al., 2000). This eolian dust flux is equivalent to a sedimentation rate of ~10 mm/ka (Rutten et al., 2000) which is negligible compared to the total sedimentation rate of ~600 mm/ka in our study area, the Gulf of Taranto (Fig. 2). Therefore, we will not further discuss this option.

For the Holocene period, sea level change as well as partly related changes in current regimes may influence the sediment composition and deposition. Transport and accumulation of sediment in the Gulf of Taranto are thought to be highly dependent on bottom currents, which vary seasonally and inter-annually along the western Adriatic coast (Milligan and Cattaneo, 2007) and in the Gulf of Taranto. We will first outline the general sedimentation features for the region. Subsequently, we will discuss the constraints of the geochemical data from XRF core scanning as proxies for environmental variability. Subsequently, we zoom in on two cores from the Gulf of Taranto and discuss differences and changes in circulation using geochemical proxies.

5.1. Sedimentation in the Gulf of Taranto region

The Ca/Ti trends across the shelf are similar for data from XRF-core scanners and ICP-AES (Fig. 3c). This confirms the robustness of the Ca/Ti ratio for assessing a stratigraphic framework for the Gallipoli Shelf sediments (Fig. 4, Supplementary material). Sedimentation rates generally decrease with depth in each core, partly due to compaction, although not to the same extent for all cores. The average sedimentation rate varies between 0.49 mm/yr (GeoB10704) and 0.92 mm/yr (GeoB10706). This indicates that the seafloor structure and the sediment accumulation in the Gulf of Taranto may be rather heterogeneous (Rossi et al., 1983; Fig. 1). This may relate to areas with enhanced non-steady-state deposition as indicated by Multibeam acoustic studies (A. Savini person. commun.) and shows that the sedimentation is not as uniform as initially anticipated and as suggested by previous studies (Cini Castagnoli et al., 1990). The latter study also identified several tephra layers from volcanic eruptions as thin horizons in the sediments

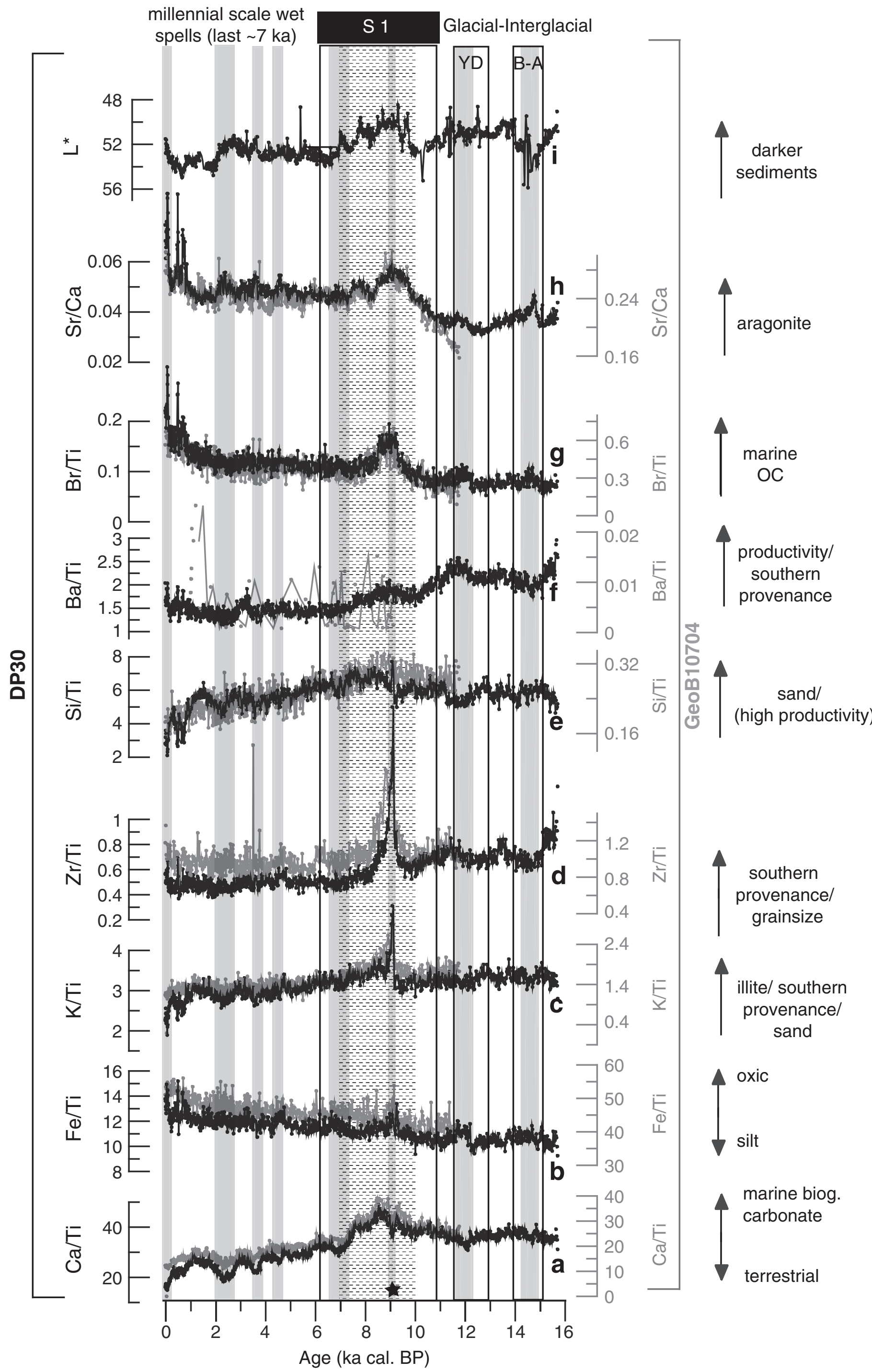

Fig. 6. Comparison of selected elemental ratios from XRF core scanning a) Ca/Ti; b) Fe/Ti; c) K/Ti; d) Zr/Ti; e) Si/Ti; f) Ba/Ti; g) Br/Ti; h) Sr/Ca and i) Black–White scale (L*) of cores DP30 (AVAATECH core scanner, black lines, scale on the left) and GeoB10704 (ITRAX core scanner, gray line, scale on the right). Gray shaded intervals indicate periods with high detrital input (low Ca/Ti); dark-gray shaded box corresponds to the interval which contains an increased amount of black particles. B–A (B–A (a/Ti); dar), YD (Younger Dryas), S1 (sapropel S1 as defined by de Lange et al., 2008). Star indicates the possible tephra layer of the Mercato eruption.

from the Gulf of Taranto over the past 2000 years. These authors used the number of pyroxene grains in the sediment to identify volcanic eruptions in the area. These volcanic events are restricted to thin layers of <0.5 cm i.e. below the resolution of our XRF data, and represent at most a minor fraction of the total sediment for regular 0.25 cm interval samples or for a 1 cm XRF scan interval. Therefore, it is concluded that with the methods used in this study it is not possible to identify such tephra layers. An exception to this is possibly an event around 9 cal. ka BP (cf. Section 5.3.2).

Although the sediments of DP23, located in the western Gulf of Taranto, are influenced by the same anticlockwise circulation within the Gulf, direct river discharge into the central and western Gulf of Taranto leads to a different chemical composition (Buccolieri et al., 2006; Goudeau et al., 2013) and sediment accumulation rate compared to the eastern part (Figs. 1 and 5). Such dominant local sources are virtually absent in the eastern Gulf (Fig. 1) and material may thus predominantly originate from more distal terrestrial and marine sources. The sediments in core DP20, located in the central Ionian Sea, also have a very different composition compared to those in the eastern Gulf (Fig. 5). This indicates that the major sediment supply to the eastern Gulf of Taranto originates from the Adriatic Sea (cf. Goudeau et al., 2013). The sediment composition in the southern Adriatic Sea (DP39) is very similar to that in the eastern Gulf of Taranto, which is another indication for a common source of the sediments in these two areas (Fig. 5). In addition, surface samples in the Gulf of Taranto consist of relatively fine-grained sediments which concords with a distal source (e.g., Weltje and Brommer, 2011). Hence, the transport and deposition of sediments are influenced by a combination of regional and more remote terrestrial and marine environmental parameters. The good correspondence between sediments from the Adriatic Sea and the Gulf of Taranto, in combination with the fine grained sediments, all indicate that only small contributions of sediment may come from local sources (Goudeau et al., 2013). This is in agreement with minor local run-off in the eastern Gulf of Taranto.

Therefore, we now focus the discussion on sediments from the eastern Gulf of Taranto, potentially reflecting supra-regional variability and being influenced by more remote and more general, prevailing paleoclimatic and hydrological conditions. Furthermore, the nearly identical patterns in geochemical composition across the Gallipoli Shelf (Figs. 4 and 6) validate the use of one core to reconstruct Holocene environmental variability for the central Mediterranean area.

5.2. Elemental ratios as a proxy for environmental variability

The geochemical composition of surface sediments in the southern Adriatic Sea and Gulf of Taranto reflect changes in grain size, productivity, and provenance (Spagnoli et al., 2008; Weltje and Brommer, 2011; Goudeau et al., 2013). Geochemical data from XRF core scanning has been used successfully to reconstruct environmental variability (e.g., Haug et al., 2001; Richter et al., 2006; Hennekam and De Lange, 2012). However, proxies are usually not affected by a single parameter, and the dominating parameter may differ per region and time interval, especially in a complex area such as the Gulf of Taranto.

5.2.1. Detrital fluxes vs. marine biogenic fluxes

The stratigraphic framework of this study is based on patterns of Ca/Ti ratios, which have been used as an indicator of marine biogenic carbonate versus terrestrial input (Richter et al., 2006; Rothwell and Rack, 2006). Although sediments from the Apulian margin contain carbonate (Pigorini, 1968), their contribution to sediments of the Gallipoli Shelf is considered to be minor at most. The values of Al (%), from detrital aluminosilicates (i.e., clay minerals), and Ca (%) mainly from marine carbonate in surface sediments from the study area fit to a Ca–Al mixing line (Goudeau et al., 2013). Thus, when sediments are enriched in clay minerals they are depleted in carbonates and vice versa. Samples from the western Gulf of Taranto deviate from this simple Ca–Al mixing line due to differing local terrestrial provenance (Goudeau et al., 2013). Hence, the Ca/Ti ratio is a valuable proxy for the variations in marine biogenic carbonate and terrestrial input into the eastern Gulf of Taranto.

5.2.2. Productivity

The Br/Ti, Si/Ti and Ba/Ti ratios are amongst the reported proxies for paleoproductivity (e.g., Rothwell and Rack, 2006; Ziegler et al., 2008). Furthermore, enhanced Sr/Ca values indicate the presence of high-Sr aragonite, and therefore, usually are linked to shallow water biogenic carbonate, thus to carbonate productivity. Increased paleoproductivity and decreased oxygen exposure time of the organic matter, lead to higher preservation of marine organic matter which is highly associated with the Br/Ti ratio (Ziegler et al., 2008). High levels of Si/Ti may indicate the presence of quartz, but can also indicate increased opal concentrations, and thus diatom accumulation. The abundance of diatoms is associated with increased paleoproductivity, as has been reported for deep Mediterranean sediments during sapropel times (Kemp et al., 1999). As silica is highly undersaturated in the oligotrophic Mediterranean waters the preservation of opal seems unlikely at the core site at the present. However, some opal may remain, when productivity and sedimentation rates are high. Therefore, we assume the Si/Ti to be mainly related to changes in grain size, i.e. quartz content, but with some potential influence of diatom productivity.

The Ba/Ti ratio is like the Ba/Al ratio, a potential indicator for paleoproductivity (Reitz et al., 2004; Thomson et al., 2006). This ratio is influenced by two major components: 'detrital' and 'biogenic' (e.g., Klump et al., 2000; Reitz et al., 2004). The detrital component is strongly influenced by river source/provenance, whereas the biogenic component is related to marine primary productivity, i.e. to $\%C_{org}$. In our study area, barium is likely to vary with changing sediment provenance as the sites are strongly influenced by a variety of terrestrial sources. Furthermore, the accumulation rate of biogenic barite increases with water depth, as part of on-going diagenetic formation processes (e.g., Dymond et al., 1992; Von Breymann et al., 1992), and thus may be low- or even absent at shallow sites like the Gulf of Taranto. Hence, we consider the Ba/Ti ratio in these sediments to be predominantly related to provenance (see Section 5.2.2).

5.2.3. Provenance and grain size

Sediments from southern Italy are elevated in K and Zr, and to a lesser extent in Ba and Fe compared to sediments from northern Italy (Cocco, 1976; Spagnoli et al., 2008; Goudeau et al., 2013). Variability in the K/Ti, Zr/Ti, Ba/Ti and Fe/Ti, therefore, at least partly reflects variance in provenance of the sediments, the higher values being associated to a more southern source. However, in the study area K/Ti and Ba/Ti are also positively correlated with grain size. Elevated Fe/Ti, K/Ti and Zr/Ti have been associated with coarser grain size as well as with changes in provenance (e.g., Rothwell and Rack, 2006). For the surface sediments in the Gulf of Taranto and southern Adriatic Sea, the Fe/Al and thus the Fe/Ti ratio are correlated to the clay and sand fractions, while K/Al (K/Ti) and Zr/Al (Zr/Ti) are positively correlated to the sand fraction only (Goudeau et al., 2013). Some of these proxies are not only affected by grain size and provenance, but also by other parameters: Fe/Ti partly reflects changes in the redox state as in more suboxic environments; Fe is mobilized in the sediments (Rothwell and Rack, 2006). In addition, climate may be reflected in the K/Ti ratio. K/Ti values are usually high in sediments that have a relatively high illite content. In general, more illite is eroded in cold environments. Here physical weathering is more dominant compared to tropical humid environments where chemical weathering dominates (Bonatti and Gartner, 1973, Yarincik et al., 2000).

Therefore, we consider the Fe/Ti, Ba/Ti, Zr/Ti, and K/Ti as proxies for provenance but with a potential impact of grain size. In addition, Fe/Ti may reflect redox conditions, while K/Ti may relate to illite content.

5.3. Reconstruction of environmental variability during the last 16 ka

During the Glacial–Interglacial transition and the subsequent Holocene, distinctly different climates occurred. In addition, considerable variability has taken place on millennial to decadal time-scales. To highlight related transitions and variability in our cores, we will focus the discussion on three periods: firstly *the Glacial–Interglacial transition* (16–10.8 *cal. ka BP*), secondly the most-recent *sapropel*: *S1/Saharan humid period* (10.8–7 *cal. ka BP*), and thirdly the *Late Holocene* (7–0 *cal. ka BP*) *period*.

5.3.1. Glacial–Interglacial transition (16–10.8 cal. ka BP)

5.3.1.1. Transition from the Last Glacial to the Bølling–Allerød. The transition from the Last Glacial to the Bølling–Allerød (B–A, ~16–14 cal. ka BP) is generally characterized by a rapid change to warmer and wetter conditions in the Mediterranean region (Rossignol-Strick, 1999; Frisia et al., 2005; Bar-Matthews and Ayalon, 2011; Giraudi et al., 2011). The Ca/Ti ratio, an indicator of biogenic carbonate versus terrestrial input (see Section 5.2.1), remains constant until ~10.8 cal. ka BP (Fig. 6a), similar to other proxies of terrestrial provenance and marine productivity such as the K/Ti, Fe/Ti, Br/Ti and the Sr/Ca ratios (Fig. 6a–h). All these elemental ratios indicate that the influence of marine and terrestrial sources remained stable during this period. Remarkably, the Ba/Ti and Zr/Ti ratios show a sharp decrease in DP30 from 16 to 14.5 cal. ka BP (Fig. 6d, f) indicating an enhanced contribution from low-Ba/Ti northern river sources, but could also be a result of a decrease in grain size. The latter may be related to a more distal provenance or to reduced winnowing at the coring site. Higher current velocities would have increase the relative amount of coarse sediment and heavy minerals such as barite during periods of decreased water depth at the DP30 core site caused by low sea level stands. Taking the low sea level into account (Grant et al., 2012), the estimated water depth at 15 cal. ka BP at our core location was 160 m. However, if we consider the Si/Ti ratio to be an indicator for quartz content or coarseness of the sediment, then the slightly increasing Si/Ti values over the same time interval between 16 and 15 cal. ka BP are inconsistent with a decrease in winnowing (Fig. 6e). In addition, if winnowing would play a role, we would expect K/Ti and Fe/Ti to also co-vary, which they do not. (Fig. 6b, c). Therefore, we conclude that the values for Ba/Ti and Zr/Ti, decreasing from 16 to 14.5 cal. ka BP, are related to an increased contribution from northern relative to southern Adriatic rivers (Goudeau et al., 2013). The lack of decreasing K/Ti values can be explained by a relation of the K/Ti values and change in relative illite content (e.g., Yarincik et al., 2000). Illite is higher in sediments from northern rivers, but it is suggested that more illite is eroded under cold and arid conditions (cf. Section 5.2). The increasing influence from northern rivers as reflected by the decreasing Ba/Ti and Zr/Ti values is coherent with a more humid climate for northern Italy (e.g., Frisia et al., 2005; Giraudi et al., 2011).

5.3.1.2. The Bølling–Allerød and Younger Dryas. The stable Ca/Ti values are interrupted by two short intervals (around 14.5 and 12.3 cal. ka BP) with higher river-fluxes (low Ca/Ti and high Fe/Ti), and increased productivity and C_{org}-fluxes (enhanced Br/Ti ratios; Fig. 6g). These intervals correspond to the Bølling–Allerød (B–A; ~14.67 cal. ka BP) and the Younger Dryas (YD; 12.9 to 11.5 cal. ka BP). During the B–A, Ba/Ti and Zr/Ti values are low compared to the YD (Fig. 6d, f). This indicates that during the YD sediments had a more southern provenance.

The short period when Ca/Ti is low in our record (12.4–12.1 cal. ka BP) is coeval with a cold spell in the GISP2 oxygen isotope ice core-record (Fig. 7a, g; Grootes and Stuiver, 1997).

In contrast to the B–A, which is characterized as warm and wet, the YD has been described as cold and dry in Italy (e.g., Bottema, 1995; Zonneveld, 1996; Frisia et al., 2005). Other records from southern Italy recording the YD are scarce and lack high resolution to confirm our observation (e.g., Combourieu-Nebout et al., 1998; Allen et al., 2002). However, high resolution pollen records from the southern Balkan and the Aegean Sea suggest that the YD can be divided into three intervals (Bordon et al., 2009; Dormoy et al., 2009). The authors show that the cold and dry YD period is interrupted by a period where warmer and more humid conditions prevailed. They observe however that winter precipitation remained low and that summer precipitation could have been similar or even higher than today. In our data we observe a drop in Ca/Ti. This is consistent with the warmer and wetter period observed by Bordon et al. (2009) and Dormoy et al. (2009). The latter relate these changing conditions to the southern emplacement of the high pressure cell of the Intertropical Convergence Zone during the YD. Today, the more northern emplacement of this zone during summer, blocks the moisture-rich westerlies, which results in the characteristic dry summer conditions (Piervitali et al., 1997; Alpert et al., 2006).

Elevated sediment erosion and therefore increased terrestrial supply to the Gulf of Taranto due to short, but intensive rainfall after long arid periods is known from the southern rivers (Piccarreta et al., 2011). Hence, it is plausible that during this warmer interval of the YD terrestrial run-off from southern Italian rivers was higher, whereas riverine input in northern and central Italy was lower.

5.3.2. Sapropel S1–Saharan humid period (10.8–7 ka BP)

The formation of the most recent sapropel S1 occurred synchronously in the deeper parts of the eastern Mediterranean between 10.8 and 6.1 cal. ka BP (De Lange et al., 2008). The higher amount of black organic particles (L*), the higher Br/Ti ratio (10–8 cal. ka BP) and Sr/Ca ratio (10.5–7.5 cal. ka BP) all mainly coincide with the older part of sapropel formation time (Fig. 6g, h, i). At these shallow and high sedimentation rate sites, Ba/Ti cannot be used as a proxy for productivity but rather for provenance. The step-wise decrease of Ba/Ti during this period therefore reflects an increase in northern provenance of the sediments rather than a decrease in productivity. The increase in organic matter content as deduced from the enhanced Br/Ti, can thus be related to an increase in preservation and productivity. In general, the period corresponding to sapropel formation is considered wet in the northern borderlands (Kotthoff et al., 2008; Giraudi et al., 2011 and references within). The high Ca/Ti ratio seems to contradict these observations (Fig. 6a). However, a high Sr/Ca ratio and a relatively enhanced $CaCO_3$ (high Ca/Ti) content in near-coastal deposits of sapropel S1 have been reported in a variety of cores from the eastern Mediterranean, and have been attributed to an increased aragonite content from a shallow-water biogenic source or to diagenetic processes for deep-basin deposits (Thomson et al., 2004; Reitz and De Lange, 2006). In view of the elevated Br/Ti, Si/Ti and Sr/Ca ratios, an enhanced organic matter-, opal-, and carbonate-productivity seems likely for this period (Fig. 6e, g, h).

The pronounced shifts observed at ~9 cal. ka BP for Fe/Ti, K/Ti, and Zr/Ti may be related to tephra from a volcanic event, and to a shift or rerouting of sediment provenance (Fig. 6b, c, d). As the sediment interval of enhanced elemental ratios is much thicker than usually found for a tephra (cf. Section 5.1) both options are possible. The tephra may be related to a series of eruptions known as the Mercato eruption (Mele et al., 2010), that resulted in distinctive, relatively thick tephras in the northern Ionian Sea (Caron et al., 2012). In addition, a potential provenance rerouting is, however, also possible as during this time sea-level rise, and flooding of the northern Adriatic occurred (Fig. 7c, h).

Often it is found that sapropel S1 is interrupted by the so called 8.2 ka cooling event (Rohling et al., 1997; De Rijk et al., 1999). This cold event is expressed in our record by enhanced marine influence and/or dry conditions (high Ca/Ti), and enhanced marine organic matter (high Br/Ti) (Figs. 6b, g and 7a).

Gallipoli Shelf sediments from the upper sapropel S1 formation period, i.e. 7.5–6.1 cal. ka BP do not show any evidence for environmental changes in the records of Br/Ti or black organic particles (Fig. 6g, i). This could be due to post-depositional oxidation of organic matter or to diminished 'sapropelic conditions' for shallow sediments during that period (e.g., van Santvoort et al., 1997). Various authors have claimed that sapropel formation at shallower sites in the Adriatic Sea stopped earlier than at deeper sites (resp. ~7.5 ka and ~6.1 ka BP; Piva et al., 2008; De Lange et al., 2008). This is thought to be related to postglacial sea-level rise, the consequent flooding of the northern Adriatic, and the related onset of NAdDW, ventilating shallower bottom waters (Piva et al., 2008). The enhanced ventilation and concomitantly reduced primary productivity and preservation are thought to have resulted in the suppression of detectable sapropel indicators in our shallow sediments of the eastern Gulf of Taranto.

5.3.3. Late Holocene (7–0 cal. ka BP)

The decrease in the Ca/Ti, Ba/Ti and Si/Ti ratio and the increase in the Fe/Ti ratio for both cores indicate a progressive increase in terrestrial input from a distal source during the mid-to-late Holocene (8.2–2.5 cal. ka BP; Figs. 6a, b, e, f and 7a). The most rapid increase in terrestrial input occurs at ~7 cal. ka BP and coincides with sea level rise (Fig. 7h; Grant et al., 2012) and the onset of NAdDW-formation,

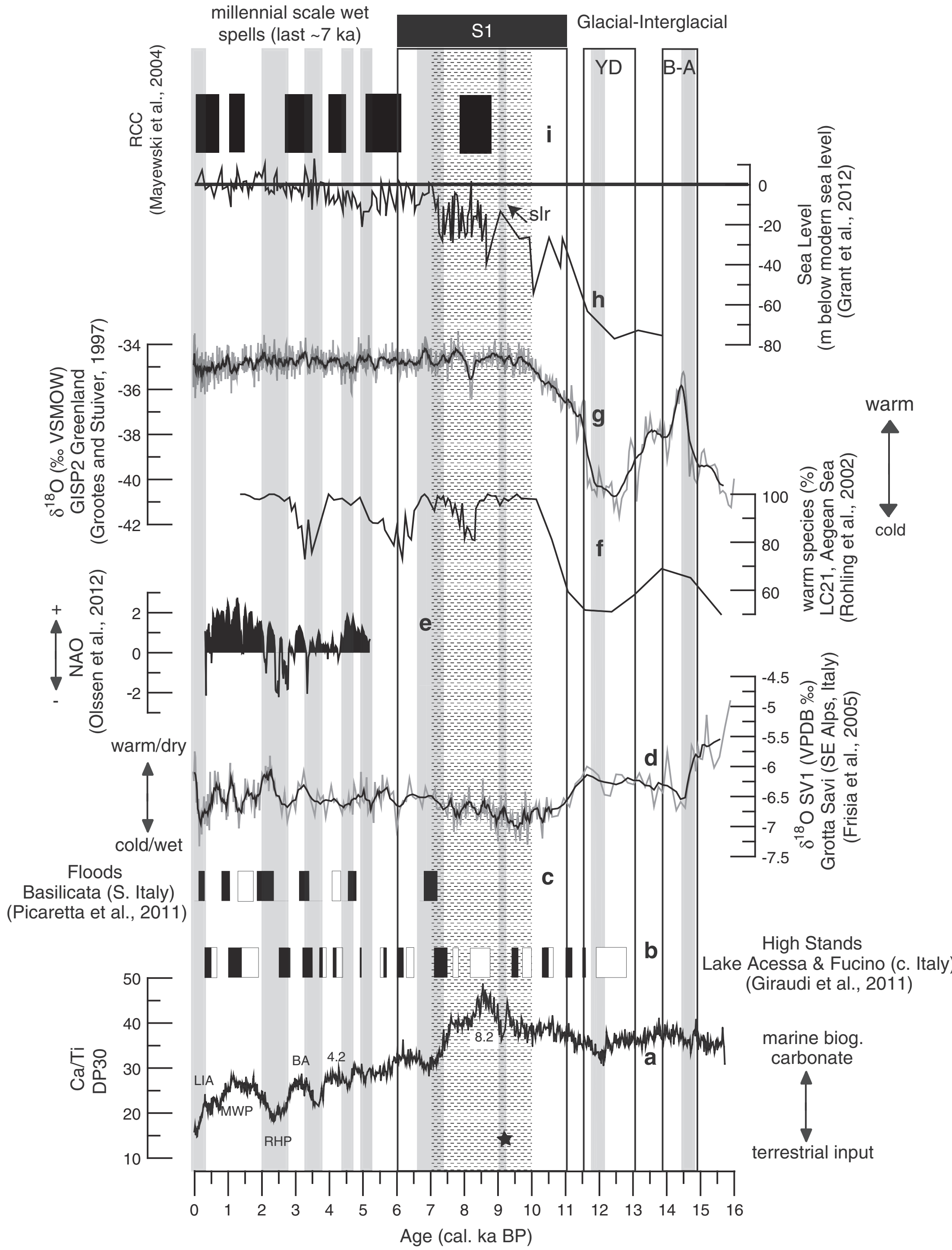

Fig. 7. a) Ca/Ti ratio of DP30 compared to: b) lake level high (black blocks) and low (gray blocks) stands of Lake Accesa and Lake Fucino, Central Italy (Giraudi et al., 2011); c) periods of increased flood frequency in the Basillicata region, South Italy (Piccarreta et al., 2011); gray blocks indicate potential summer flood events; d) speleothem oxygen isotope record from Grotta Savi, SE Alps, Italy (Frisia et al., 2005); e) reconstruction of the NAO from a lake in Greenland (Olsen et al., 2012); f) percentage of warm water foraminifera in the Aegean Sea (Rohling et al., 2002); g) the GISP2 oxygen isotope record by Grootes and Stuiver (1997); h) reconstruction of sea level variability (Grant et al., 2012) and i) rapid climate change events (Mayewski et al., 2004). Gray shaded boxes indicate periods of high detrital input (low Ca/Ti); gray shaded box marks the interval with an increased amount of black particles (see Fig. 6i). B–A (Bølling–Allerød), YD (Younger Dryas), S1 (sapropel S1 as defined by de Lange et al., 2008), 8.2 (8.2 ka event), 4.2 (4.2 ka event), BA (Bronze Age), RHP (Roman Humid Period), MWP (Medieval Warm Period), LIA (Little Ice Age), star indicates the possible tephra layer of the Mercato eruption, slr indicates the sea level rise, related to flooding of the northern Adriatic Sea shelf.

enhancing the southwards transport of sediment, and presumably inducing the end of sapropel S1 formation in the southern Adriatic (De Rijk et al., 1999; Piva et al., 2008). Although there is no age model for core DP39, we observe a similar pattern in Ca/Ti in DP39 and DP30 from around 4.2 m depths onwards, corresponding to ~7 cal. ka BP in DP30 (Figs. 4 and 5). This correlation between Adriatic core DP39 and the Gulf of Taranto is consistent with a closer connection between these two areas during the period 0–7 cal. ka BP. Furthermore between 7 and 4 cal. ka BP, higher lake levels and increased flood frequency in Italy also indicate less aridity (e.g., Giraudi et al., 2011; Piccarreta et al., 2011), which is presumably related to the increased strength of the westerlies in the Mediterranean area (Fig. 7b, c). The observed increasing trend in terrestrial input thus corresponds to increased humidity that can be related to a reorganization of atmospheric circulation and hydrological patterns in the Northern Hemisphere (e.g., Haug et al., 2001; Mayewski et al., 2004; Knudsen et al., 2011). This has been attributed to changes in the orbital configuration and declining influence of continental ice sheets (e.g., Rossignol-Strick, 1985; Haug et al., 2001; Knudsen et al., 2011; Shuman and Plank, 2011). Moreover, deforestation, since 5500 years ago, possibly anthropogenic in origin, has resulted in higher sediment fluxes to the Adriatic Sea (Oldfield et al., 2003). This is in agreement with the high sedimentation rates and low Ca/Ti found in the upper part of DP30 which is thought to reflect enhanced deforestation especially during the last 700 years (Oldfield et al., 2003).

In addition to the long-term decreasing trend, Ca/Ti, K/Ti, Si/Ti and Sr/Ca ratios of the cores show oscillations with periods of ~1000–2000 years during the last 8 cal. ka BP (Figs. 6a, c, e, h and 7a). Intervals of low Ca/Ti (high detrital input), low K/Ti (low illite content and therefore humid conditions), low Si/Ti (lower quartz content) and high Sr/Ca (high aragonite content) ratios are observed at 7000–6500, 4900–4600, 3400–3600, 2500–2000 (RHP) and 250 cal. yr BP. These periods correspond to periods of high lake levels and increased flood frequency in central and southern Italy (Giraudi et al., 2011; Piccarreta et al., 2011; Fig. 7b, c). Some of the intervals with high lake levels and frequent floods during the MWP and around the 4.2 ka event seem to have no expression in the Ca/Ti ratios of this study (Fig. 7a). However, Piccarreta et al. (2011) describe the observed floods during these particular periods as low-frequency, high-precipitation events, i.e. storms not related to mean annual rain fall (Fig. 7c). Furthermore, although lake levels are higher during these periods, they are not as pronounced as the other lake level high stands (Giraudi et al., 2011). In addition, Magny et al. (2003, 2009) have shown that the 4.2 ka event has a complex pattern of short wet and dry periods, which are not synchronous across the Mediterranean basin. A minor annual impact, low frequency, and complex nature of these wet spells can explain why they left no clear signal in the sediments of the Gulf of Taranto. Although, deforestation may play a role in the high sedimentation rates of the last 5500 years, this cannot explain the observed patterns of wet/dry spells in this study (Oldfield et al., 2003). In addition, human impact in the environment appears to be very restricted in southern Italy during the late Holocene (Di Rita and Magri, 2009). Therefore, we assume that climatic variability must have been the major factor influencing the element composition.

With regard to large-scale climate events, the observed dry spells (high Ca/Ti) at ~6500–5000,4500–3600, 3400–2500 (Bronze Age (BA)) and 2000–1000 (MWP) cal. yr BP, correspond to globally recognized, so called ‘cool poles, dry tropics’ rapid climate change (RCC) events (Mayewski et al., 2004, Fig. 7i). These events are also observed in the northern and central Adriatic Sea (Piva et al., 2008). The comparison of the Ca/Ti ratio to the Aegean cold spells (Fig. 7f; Rohling et al., 2002) demonstrates that increased run-off (low Ca/Ti ratio) can be found near the beginning and end of Aegean and Adriatic cold spells (De Rijk et al., 1999). Frisia et al., 2005, based on a stalagmite record, suggested relatively high temperatures in northern Italy during these ‘wet’ periods. Holocene cold spells as observed at 2.7 (BA), 6 and 8.2 cal. ka BP in the Aegean Sea and Adriatic Sea have been related to outbreaks of cold, dry winds from Siberia, known as the Bora in the Adriatic region, and fit to maximum alpine glacier extent and deep Icelandic Lows (Denton and Karlén, 1973; Rohling et al., 2002; Mayewski et al., 2004; Fig. 7f). Today deep Icelandic Lows are related to a more positive NAO, hence dryer and colder conditions in the Mediterranean region (Hurrell, 1995; Brandimarte et al., 2011, Fig. 7e). A persistent positive winter NAO is also inferred for the other RCC events (MWP and 4.2 ka event), in particular the MWP (Lamy et al., 2006; Trouet et al., 2009; Nieto-Moreno et al., 2011; Olsen et al., 2012, Fig. 7e). The positive state of the NAO today has been related to low Sea Surface Temperatures in the North Atlantic and higher temperatures in Greenland (e.g., Hurrell, 1995). This pattern is, however, neither evident in Icelandic Low reconstructions, nor in the Aegean cold spells (Rohling et al., 2002). Rohling et al. (2002) suggest that the absence of some RCC in the Aegean Sea record is related to the attenuated forcing of ice-related feedback mechanisms since ~7 ka, affecting only sites directly influenced by the thermohaline circulation during relatively ‘weak’ and less widely recognized events as the MWP and the 4.2 ka event.

In summary, periods with high Ca/Ti ratio correspond to a positive NAO, hence dryer and colder conditions (Fig. 7a and e). We therefore suggest that periods of increased detrital input can be associated with a negative NAO, inducing humid and marginally warmer conditions in the Mediterranean region (e.g. Hurrell, 1995; Trigo et al., 2006). Although the increased detrital input during the LIA (~650–150 cal. yr BP) seems to contradict the patterns found during other periods between ~9000 and 600 cal. yr BP, it should be noted that most increased run-off is visible at the end of the LIA (~250 cal. yr BP–150 cal. yr BP), which is in agreement with reconstructions of western Mediterranean climate and NAO variability (e.g., Trouet et al., 2009; Nieto-Moreno et al., 2011).

Besides the NAO, also local factors have an influence on river run-off in the Mediterranean (Lionello et al., 2006). First, during dry periods that lack cold Bora winds (i.e. the MWP and 4.2 ka event) it is relatively warm compared to the other RCC events (Frisia et al., 2005). This results in increased evaporation in the Italian hinterland and possibly contributes to reduced run-off. Secondly, less ADW is formed during warmer intervals (Turchetto et al., 2007). This leads to increased influence of the Levantine Intermediate Water (LIW) from the central Ionian Sea, and thus to a higher marine influence into the study area (higher Ca/Ti ratios). Thirdly, at transitions from cold to warm periods, meltwater from alpine glaciers may also contribute to the observed rising river run-off.

In summary, our data show that a positive state of NAO is related to a relatively dry climate in the Mediterranean. Such conditions may be modified by regional factors such as Mediterranean circulation patterns, increased evaporation, and dry Bora winds.

6. Conclusions

On the basis of multiple XRF core scans and precise AMS ^{14}C-dating, we show that sediment cores from the Gulf of Taranto can be accurately correlated using the Ca/Ti ratio. For the sites mostly affected by supra-regional influences, we have derived climate variability for the last 16 cal. ka BP at high-resolution using a range of geochemical proxies.

In general, conditions were dry and stable during the Glacial/Interglacial transition. Two short intervals of increased detrital input can be related to the Bølling–Allerød and late Younger Dryas (YD). During the late YD, this increased detrital input appears to originate from a southern Italian source, suggesting an increased precipitation in Southern Italy, while run off from Northern Italy remained low.

On the shallow Gallipoli Shelf, slightly increased concentrations of organic material and biogenic carbonate are observed during part of the sapropel S1 period (~10–7.5 cal. ka BP) indicating increased primary productivity and/or preservation. After 7 cal. ka BP, a constant increase in terrestrial input and increased sedimentation rates indicate a progressive change towards modern circulation for the Adriatic/NW Ionian Sea. In addition, wetter conditions and deforestation during this period have resulted in increased terrestrial fluxes into the area.

Superimposed on this long-term trend, we observe millennial-scale variability in terrestrial input which corresponds to global climate variability and to the NAO in particular. Although regional factors such as increased evaporation also contribute, we suggest that a positive state of the NAO, i.e. dry conditions in the Mediterranean, dominated during RCC events such as the MWP and the Bronze Age.

Supplementary data to this article can be found online at http://dx.doi.org/10.1016/j.margeo.2013.12.003.

Acknowledgments

This contribution is part of the MOCCHA project, supported by the European Science Foundation (ESF-EuroMarc) with associated financial support from the Netherlands Organization for Scientific Research (NWO-Project .817.01.002), the German Science Foundation (DFG grants to GV and KZ), and the Swiss National Science Foundation (SNF Projects 20MA21-115934 and 200020_134987). Alessandra Savini (Milan-Bicocca University) is thanked for access to Multibeam data and discussions of sedimentary dynamics of the area. We thank Helen de Waard for her help with ICP-AES analyses at Utrecht University and Rineke Gieles for core scanning assistance at the Royal Netherlands Institute for Sea Research. Prof. Dr. Bernd Zolischka, Sabine Stahl and Christian Ohlendorf are thanked for technical support and access to XRF-ITRAX scan equipment at the Geography Institute (GEOPOLAR group), University of Bremen. Sample material has been provided by the GeoB Core Repository at the MARUM—Center for Marine Environmental Sciences, University of Bremen, Germany. The data reported in this paper are achieved in Pangaea (www.pangea.de). Authors are grateful to Captain, Crew and Colleagues with *RV Pelagia* DOPPIO-cruise (October–November 2008) and MACCHIATO-cruise (November–December 2009), both coordinated by Gert J. De Lange, and with *RV Poseidon* CAPPUCCINO-cruise (July 2006) coordinated by Karin Zonneveld. In addition, we acknowledge financial, technical, and logistic support given by NIOZ/NWO for DOPPIO and MACCHIATO cruises and the DFG for CAPPUCCINO cruise. We thank two anonymous reviewers for constructive and helpful comments.

References

Allen, J.R.M., Watts, W.A., McGee, E., Huntley, B., 2002. Holocene environmental variability—the record from Lago Grande di Monticchio, Italy. Quaternary International 88 (1), 69–80. http://dx.doi.org/10.1016/S1040-6182(01)00074-X.

Alpert, P., Baldi, M., Ilani, R., Krichak, S., Price, C., Rodó, X., Saaroni, H., Ziv, B., Kishcha, P., Barkan, J., Mariotti, A., Xoplaki, E., 2006. Chapter 2: Relations between climate variability in the Mediterranean region and the tropics: ENSO, South Asian and African monsoons, hurricanes and Saharan dust. In: Lionello, P., M.-R., P., Boscolo, R. (Eds.), Developments in Earth and Environmental Sciences. Elsevier, pp. 149–177.

Artegiani, A., Bregant, D., Paschini, N., Raicich, F., Russo, A., 1997. The Adriatic Sea general circulation. Part I: air–sea interactions and water mass structure. Journal of Physical Oceanography 27, 1492–1514.

Bar-Matthews, M., Ayalon, A., 2011. Mid-Holocene climate variations revealed by high-resolution speleothem records from Soreq Cave, Israel and their correlation with cultural changes. The Holocene 21, 163–171. http://dx.doi.org/10.1177/0959683610384165.

Bignami, F., Sciarra, R., Carniel, S., Santoleri, R., 2007. Variability of Adriatic Sea coastal turbid waters from SeaWiFS imagery. Journal of Geophysical Research 112. http://dx.doi.org/10.1029/2006JC003518 (C03S10).

Boer, W., Van, G.D., den Bergh, H., De Haas, H.C., De Stigter, R., Gieles, and Tj CE Van Weering, 2006. Validation of accumulation rates in teluk banten (Indonesia) from commonly applied ^{210}pb models, using the 1883 krakatau tephra as time marker. Marine Geology 227 (3), 263–277.

Bonatti, E., Gartner, S., 1973. Caribbean climate during Pleistocene ice ages. Nature 244, 563–565. http://dx.doi.org/10.1038/244563a0.

Bond, G., Kromer, B., Beer, J., Muscheler, R., Evans, M.N., Showers, W., Hoffmann, S., Lotti-Bond, R., Hajdas, I., Bonani, G., 2001. Persistent solar influence on north Atlantic climate during the Holocene. Science 294, 2130–2136. http://dx.doi.org/10.1126/science.1065680.

Bordon, A., Peyron, O., Lézine, A.M., Brewer, S., Fouache, E., 2009. Pollen-inferred late-glacial and Holocene climate in southern Balkans (lake Maliq). Quaternary International 200 (1), 19–30. http://dx.doi.org/10.1016/j.quaint.2008.05.014.

Bottema, S., 1995. The younger dryas in the Eastern Mediterranean. Quaternary Science Reviews 14 (9), 883–891. http://dx.doi.org/10.1016/0277-3791(95)00069-0.

Brandimarte, L., Di Baldassarre, G., Bruni, G., D'Odorico, P., Montanari, A., 2011. Relation between the North-Atlantic Oscillation and hydroclimatic conditions in Mediterranean areas. Water Resource Management 25, 1269–1279. http://dx.doi.org/10.1007/s11269-010-9742-5.

Bronk Ramsey, C., Higham, T.F.G., Brock, F., Baker, D., Ditchfield, P., 2009. Radiocarbon dates from the Oxford AMS system: Archaeometry datelist 33. Archaeometry 51, 323–349.

Buccolieri, A., Buccolieri, G., Cardellicchio, N., Dell'Atti, A., Di Leo, A., Maci, A., 2006. Heavy metals in marine sediments of Taranto Gulf (Ionian Sea, Southern Italy). Marine Chemistry 99, 227–235. http://dx.doi.org/10.1016/j.marchem.2005.09.009.

Caron, B., Siani, G., Sulpizio, R., Zanchetta, G., Paterne, M., Santacroce, R., Tema, E., Zanella, E., 2012. Late Pleistocene to Holocene tephrostratigraphic record from the Northern Ionian Sea. Marine Geology 311, 41–51. http://dx.doi.org/10.1016/j.margeo.2012.04.001.

Cattaneo, A., Correggiari, A., Langone, L., Trincardi, F., 2003. The late-Holocene Gargano subaqueous delta, Adriatic shelf: sediment pathways and supply fluctuations. Marine Geology 193, 61–91. http://dx.doi.org/10.1016/S0025-3227(02)00614-X.

Chen, L., Zonneveld, K.A.F., Versteegh, G.J.M., 2011. Short term climate variability during “Roman Classical Period” in the eastern Mediterranean. Quaternary Science Reviews 3880–3891. http://dx.doi.org/10.1016/j.quascirev.2011.09.024.

Chen, L., Zonneveld, K.A.F., Versteegh, G.J.M., 2013. Paleoclimate of the Southern Adriatic Sea region during the ‘Medieval Climate Anomaly’ reflected by organic walled dinoflagellate cysts. The Holocene 23, 645–655. http://dx.doi.org/10.1177/0959683612467482.

Cini Castagnoli, G., Bonino, G., Caprioglio, F., Provenzale, A., Serio, M., Zhu, G.-M., 1990. The carbonate profile of two recent Ionian Sea cores: evidence that the sedimentation rate is constant over the last millennia. Geophysical Research Letters 17 (11), 1937–1940. http://dx.doi.org/10.1029/GL017i011p01937.

Cini Castagnoli, G., Bonino, G., Serio, M., 1992. Common spectral features in the 5500-year record of total carbonate in sea sediments and radiocarbon in tree rings. Radiocarbon 34, 798–805.

Cini Castagnoli, G., Bernasconi, S.M., Bonino, G., Della Monica, P., Taricco, C., 1999. 700 year record of the 11 year solar cycle by planktonic foraminifera of a shallow water Mediterranean core. Helioseismology and Solar Variability 24, 233–236. http://dx.doi.org/10.1016/S0273-1177(99)00506-2.

Cocco, E., 1976. Italian North Ionian coast—tendency towards erosion. Marine Geology 21, M49–M57. http://dx.doi.org/10.1016/0025-3227(76)90057-8.

Combourieu-Nebout, N., Paterne, M., Turon, J.L., Siani, G., 1998. A high-resolution record of the last deglaciation in the central Mediterranean Sea: palaeovegetation and palaeohydrological evolution. Quaternary Science Reviews 17 (4–5), 303–317. http://dx.doi.org/10.1016/S0277-3791(97)00039-5.

Correggiari, A., Guerzoni, S., Lenaz, R., Quarantotto, G., Rampazzo, G., 1989. Dust deposition in the central Mediterranean (Tyrrhenian and Adriatic Seas): relationships with marine sediments and riverine input. Terra Nova 1, 549–558. http://dx.doi.org/10.1111/j.1365-3121.1989.tb00431.x.

Croudace, I.W., Rindby, A., Rothwell, R.G., 2006. ITRAX: Description and Evaluation of a New Multi-Function X-Ray Core Scanner. 267. Geological Society, London, Special Publications, pp. 51–63.

De Lange, G.J., Thomson, J., Reitz, A., Slomp, C.P., Speranza Principato, M., Erba, E., Corselli, C., 2008. Synchronous basin-wide formation and redox-controlled preservation of a Mediterranean sapropel. Nature Geoscience 1, 606–610. http://dx.doi.org/10.1038/ngeo283.

De Lange, G.J., 2009. and cruise participants MACCHIATO Cruise with R.V. PELAGIA to the Eastern Mediterranean.

deMenocal, P., Ortiz, J., Guilderson, T., Sarnthein, M., 2000. Coherent high- and low-latitude climate variability during the Holocene Warm Period. Science 288, 2198–2202. http://dx.doi.org/10.1126/science.288.5474.2198.

Denton, G.H., Karlén, W., 1973. Holocene climatic variations—their pattern and possible cause. Quaternary Research 3 (2), 155–205. http://dx.doi.org/10.1016/0033-5894(73)90040-9.

De Rijk, S., Hayes, A., Rohling, E.J., 1999. Eastern Mediterranean sapropel S1 interruption: an expression of the onset of climatic deterioration around 7 ka BP. Marine Geology 153, 337–343. http://dx.doi.org/10.1016/S0025-3227(98)00075-9.

Di Rita, F., Magri, D., 2009. Holocene drought, deforestation and evergreen vegetation development in the central Mediterranean: a 5500 year record from Lago Alimini Piccolo, Apulia, southeast Italy. The Holocene 19 (2), 295–306. http://dx.doi.org/10.1177/0959683608100574.

Dormoy, I., Peyron, O., Combourieu Nebout, N., Goring, S., Kotthoff, U., Magny, M., Pross, J., 2009. Terrestrial climate variability and seasonality changes in the Mediterranean region between 15 000 and 4000 years BP deduced from marine pollen records. Climate of the Past 5 (4), 615–632. http://dx.doi.org/10.5194/cp-5-615-2009.

Dymond, J., Suess, E., Lyle, M., 1992. Barium in deep-sea sediment: a geochemical proxy for paleoproductivity. Paleoceanography 7, 163–181. http://dx.doi.org/10.1029/92PA00181.

Frisia, S., Borsato, A., Spötl, C., Villa, I.M., Cucchi, F., 2005. Climate variability in the SE Alps of Italy over the past 17 000 years reconstructed from a stalagmite record. Boreas 34, 445–455. http://dx.doi.org/10.1080/03009480500231336.

Gennari, G., Tamburini, F., Ariztegui, D., Hajdas, I., Spezzaferri, S., 2009. Geochemical evidence for high-resolution variations during deposition of the Holocene S1 sapropel on the Cretan Ridge, Eastern Mediterranean. Palaeogeography, Palaeoclimatology, Palaeoecology 273, 239–248. http://dx.doi.org/10.1016/j.paleo.2008.06.007.

Giraudi, C., Magny, M., Zanchetta, G., Drysdale, R.N., 2011. The Holocene climatic evolution of Mediterranean Italy: a review of the continental geological data. The Holocene 21, 105–115. http://dx.doi.org/10.1177/0959683610377529.

Goudeau, M.-L.S., Grauel, A.-L., Bernasconi, S., De Lange, G.J., 2013. Provenance of surface sediments along the southeastern Adriatic coast off Italy: an overview. Estuarine Coastal and Shelf Science 134, 45–56. http://dx.doi.org/10.1016/j.ecss.2013.09.009.

Grant, K.M., Rohling, E.J., Bar-Matthews, M., Ayalon, A., Medina-Elizalde, M., Bronk Ramsey, C., Satow, C., Roberts, A.P., 2012. Rapid coupling between ice volume and polar temperature over the past 150,000 years. Nature 491 (7426), 744–747. http://dx.doi.org/10.1038/nature11593.

Grauel, A.-L., Leider, A., Goudeau, M.-L.S., Müller, I.A., Bernasconi, S.M., Hinrichs, K.-U., De Lange, G.J., Zonneveld, K.A.F., Versteegh, G.J.M., 2013a. What do SST really tell us? A high-resolution multiproxy ($U^{K'}_{37}$, TEXH86 and foraminifera $\delta^{18}O$) study in the Gulf of Taranto, central Mediterranean Sea. Quaternary Science Reviews 73, 115–131. http://dx.doi.org/10.1016/j.quascirev.2013.05.007.

Grauel, A.-L., Goudeau, M.-L., de Lange, G.J., Bernasconi, S.M., 2013b. Climate of the past 2500 years in the Gulf of Taranto, central Mediterranean Sea: a high-resolution climate reconstruction based on $\delta^{18}O$ and $\delta^{13}C$ of *Globigerinoides ruber* (white). The Holocene 23 (10), 1440–1446. http://dx.doi.org/10.1177/0959683613493937.

Grootes, P.M., Stuiver, M., 1997. Oxygen 18/16 variability in Greenland snow and ice with 103 to 105-year time resolution. Journal of Geophysical Research 102, 26455–26470. http://dx.doi.org/10.1029/97JC00880.

Haug, G.H., Hughen, K.A., Sigman, D.M., Peterson, L.C., Röhl, U., 2001. Southward migration of the Intertropical Convergence Zone through the Holocene. Science 293, 1304–1308. http://dx.doi.org/10.1126/science.1059725.

Hennekam, R., De Lange, G.J., 2012. X-ray fluorescence core scanning of wet marine sediments: methods to improve quality and reproducibility of high-resolution paleoenvironmental records. Limnology and Oceanography: Methods 10, 991–1003. http://dx.doi.org/10.4319/lom.2012.10.991.

Hilgen, F.J., 1991. Astronomical calibration of Gauss to Matuyama sapropels in the Mediterranean and implication for the Geomagnetic Polarity Time Scale. Earth and Planetary Science Letters 104, 226–244.

Hughen, K.A., Baillie, M.G.L., Bard, E., Beck, J.W., Bertrand, C.J.H., Blackwell, P.G., Buck, C.E., Burr, G.S., Cutler, K.B., Damon, P.E., Edwards, R.L., Fairbanks, R.G., Friedrich, M., Guilderson, T.P., Kromer, B., McCormac, G., Manning, S., Ramsey, C.B., Reimer, P.J., Reimer, R.W., Remmele, S., Southon, J.R., Stuiver, M., Talamo, S., Taylor, F.W., van der Plicht, J., Weyhenmeyer, C.E., 2004. Marine04 marine radiocarbon age calibration, 0–26 cal kyr BP. Radiocarbon 46, 1059–1086.

Hurrell, J.W., 1995. Decadal trends in the North Atlantic Oscillation: regional temperatures and precipitation. Science 269, 676–679. http://dx.doi.org/10.1126/science.269.5224.676.

Jilbert, T., Reichart, G.-J., Aeschlimann, B., Gunther, D., Boer, W., De Lange, G., 2010a. Climate-controlled multidecadal variability in North African dust transport to the Mediterranean. Geology 38, 19–22. http://dx.doi.org/10.1130/G25287.1.

Jilbert, T., Reichart, G.J., Mason, P., De Lange, G.J., 2010b. Short-time-scale variability in ventilation and export productivity during the formation of Mediterranean sapropel S1. Paleoceanography 25. http://dx.doi.org/10.1029/2010PA001955 (PA4232).

Joannin, S., Brugiapaglia, E., de Beaulieu, J., Bernardo, L., Magny, M., Peyron, O., Goring, S., Vannière, B., 2012. Pollen-based reconstruction of Holocene vegetation and climate in southern Italy: the case of Lago Trifoglietti. Climate of the Past 8, 1973–1996. http://dx.doi.org/10.5194/cp-8-1973-2012.

Kemp, A.E., Pearce, R.B., Koizumi, I., Pike, J., Rance, S.J., 1999. The role of mat-forming diatoms in the formation of Mediterranean sapropels. Nature 398 (6722), 57–61. http://dx.doi.org/10.1038/18001.

Klump, J., Hebbeln, D., Wefer, G., 2000. The impact of sediment provenance on barium-based productivity estimates. Marine Geology 169, 259–271.

Knudsen, M.F., Seidenkrantz, M.-S., Jacobsen, B.H., Kuijpers, A., 2011. Tracking the Atlantic Multidecadal Oscillation through the last 8,000 years. Nature Communications 2, 178. http://dx.doi.org/10.1038/ncomms1186.

Kotthoff, U., Pross, J., Müller, U.C., Peyron, O., Schmiedl, G., Schulz, H., Bordon, A., 2008. Climate dynamics in the borderlands of the Aegean Sea during formation of sapropel S1 deduced from a marine pollen record. Quaternary Science Reviews 27 (7), 832–845. http://dx.doi.org/10.1016/j.quascirev.2007.12.001.

Lamy, F., Arz, H.W., Bond, G.C., Bahr, A., Pätzold, J., 2006. Multicentennial-scale hydrological changes in the Black Sea and northern Red Sea during the Holocene and the Arctic/North Atlantic Oscillation. Paleoceanography 21. http://dx.doi.org/10.1029/2005PA001184 (PA 1008).

Lionello, P., Malanotte-Rizzoli, P., Boscolo, R., Alpert, P., Artale, V., Li, L., Luterbacher, J., May, W., Trigo, R., Tsimplis, M., Ulbrich, U., Xoplaki, E., 2006. The Mediterranean climate: an overview of the main characteristics and issues. In: Lionello, P., M.-R., P., Boscolo, R. (Eds.), Developments in Earth and Environmental Sciences. Elsevier, pp. 1–26.

Lourens, L.J., Antonarakou, A., Hilgen, F.J., Van Hoof, A.A.M., Vergnaud-Grazzini, C., Zachariasse, W.J., 1996. Evaluation of the Plio-Pleistocene Astronomical Timescale. Paleoceanography 11, 391–413. http://dx.doi.org/10.1029/96PA01125.

Magny, M., Bégeot, C., Guiot, J., Peyron, O., 2003. Contrasting patterns of hydrological changes in Europe in response to Holocene climate cooling phases. Quaternary cience Reviews 22 (15), 1589–1596. http://dx.doi.org/10.1016/S0277-3791(03)00131-8.

Magny, M., Vannière, B., Zanchetta, G., Fouache, E., Touchais, G., Petrika, L., Coussot, C., Walter-Simonnet, A.-V., Arnaud, F., 2009. Possible complexity of the climatic event around 4300–3800 cal. BP in the central and western Mediterranean. The Holocene 19, 823–833. http://dx.doi.org/10.1177/0959683609337360.

Malinverno, E., Taviani, M., Rosso, A., Violanti, D., Villa, I., Savini, A., Vertino, A., Remia, A., Corselli, C., 2010. Stratigraphic framework of the Apulian deep-water coral province, Ionian Sea. Deep Sea Research Part II 57, 345–359. http://dx.doi.org/10.1016/j.dsr2.2009.08.025.

Mayewski, P.A., Rohling, E.E., Curt Stager, J., Karlén, W., Maasch, K.A., David Meeker, L., Meyerson, E.A., Gasse, F., van Kreveld, S., Holmgren, K., Lee-Thorp, J., Rosqvist, G., Rack, F., Staubwasser, M., Schneider, R.R., Steig, E.J., 2004. Holocene climate variability. Quaternary Research 62, 243–255. http://dx.doi.org/10.1016/j.yqres.2004.07.001.

Mele, D., Sulpizio, R., Dellino, P., La Volpe, L., 2010. Stratigraphy and eruptive dynamics of a long-lasting Plinian eruption of Somma–Vesuvius: the Pomici di Mercato (8900 years BP). Bulletin of Volcanology 73, 257–278. http://dx.doi.org/10.1007/s00445-010-0407-2.

Milligan, T.G., Cattaneo, A., 2007. Sediment dynamics in the western Adriatic Sea: from transport to stratigraphy. Continental Shelf Research 27, 287–295. http://dx.doi.org/10.1016/j.csr.2006.11.001.

Nieto-Moreno, V., Martínez-Ruiz, F., Giralt, S., Jiménez-Espejo, F., Gallego-Torres, D., Rodrigo-Gámiz, M., García-Orellana, J., Ortega-Huertas, M., De Lange, G.J., 2011. Tracking climate variability in the western Mediterranean during the Late Holocene: a multiproxy approach. Climate of the Past 7, 9. http://dx.doi.org/10.5194/cp-7-1395-2011.

Oldfield, F., Asioli, A., Accorsi, C.A., Mercuri, A.M., Juggins, S., Langone, L., Rolph, T., Trincardi, F., Woff, G., Gibbsa, Z., Vigliotti, L., Frignani, M., van der Post, K., Branch, N., 2003. A high resolution late Holocene palaeo environmental record from the central Adriatic Sea. Quaternary Science Reviews 22 (2), 319–342. http://dx.doi.org/10.1016/S0277-3791(02)00088-4 (doi: http://dx.doi.org/10.1016/S0277-3791(02)00088-4).

Olsen, J., Anderson, N.J., Knudsen, M.F., 2012. Variability of the North Atlantic Oscillation over the past 5200 years. Nature Geoscience 5, 808–812. http://dx.doi.org/10.1038/ngeo1589.

Paillard, D., Labeyrie, L., Yiou, P., 1996. Macintosh program performs time-series analysis. Eos, Transactions American Geophysical Union 77, 379.

Piccarreta, M., Caldara, M., Capolongo, D., Boenzi, F., 2011. Holocene geomorphic activity related to climatic change and human impact in Basilicata, Southern Italy. Geomorphology 128, 137–147. http://dx.doi.org/10.1016/j.geomorph.2010.12.029.

Piervitali, E., Colacino, M., Conte, M., 1997. Signals of climatic change in the Central–Western Mediterranean Basin. Theoretical and Applied Climatology 58 (3-4), 211–219. http://dx.doi.org/10.1007/BF00865021.

Pigorini, B., 1968. Sources and dispersion of recent sediments of the Adriatic Sea. Marine Geology 6 (3), 187–229. http://dx.doi.org/10.1016/0025-3227(68)90031-5.

Piva, A., Asioli, A., Trincardi, F., Schneider, R.R., Vigliotti, L., 2008. Late-Holocene climate variability in the Adriatic Sea (Central Mediterranean). The Holocene 18, 153–167. http://dx.doi.org/10.1177/0959683607085606.

Poulain, P.-M., 2001. Adriatic Sea surface circulation as derived from drifter data between 1990 and 1999. Journal of Marine Systems 29, 3–32.

Reimer, P.J., Baillie, M.G.L., Bard, E., Bayliss, A., Beck, J.W., Bertrand, C.J.H., Blackwell, P.G., Buck, C.E., Burr, G.S., Cutler, K.B., Damon, P.E., Edwards, R.L., Fairbanks, R.G., Friedrich, M., Guilderson, T.P., Hogg, A.G., Hughen, K.A., Kromer, B., McCormac, G., Manning, S., Ramsey, C.B., Reimer, R.W., Remmele, S., Southon, J.R., Stuiver, M., Talamo, S., Taylor, F.W., van der Plicht, J., Weyhenmeyer, C.E., 2004. IntCal04 terrestrial radiocarbon age calibration, 0–26 cal kyr BP. Radiocarbon 46, 1029–1058.

Reitz, A., De Lange, G.J., 2006. Abundant Sr-rich aragonite in eastern Mediterranean sapropel S1: diagenetic vs. detrital/biogenic origin. Palaeogeography, Palaeoclimatology, Palaeoecology 235, 135–148. http://dx.doi.org/10.1016/j.palaeo.2005.10.024.

Reitz, A., Pfeifer, K., De Lange, G.J., Klump, J., 2004. Biogenic barium and the detrital Ba/Al ratio: a comparison of their direct and indirect determination. Marine Geology 204, 289–300. http://dx.doi.org/10.1016/S0025-3227(04)00004-0.

Richter, T.O., van der Gaast, S., Koster, B., Vaars, A., Gieles, R., de Stigter, H.C., de Haas, H., van Weering, T.C.E., 2006. The Avaatech XRF Core Scanner: technical description and applications to NE Atlantic sediments. In: Rothwell, G. (Ed.), New Techniques in Sediment Core Analysis. Geological Society London Special Publication (39-11).

Rohling, E.J., Jorissen, F.J., De Stigter, H.C., 1997. 200 Year interruption of Holocene sapropel formation in the Adriatic Sea. Journal of Micropalaeontology 16, 97–108. http://dx.doi.org/10.1144/jm.16.2.97.

Rohling, E.J., Mayewski, P.A., Abu-Zied, R.H., Casford, J.S.L., Hayes, A., 2002. Holocene atmosphere–ocean interactions: records from Greenland and the Aegean Sea. Climate Dynamics 18, 587–593. http://dx.doi.org/10.1007/s00382-001-0194-8.

Rossi, S., Auroux, C., Mascle, J., 1983. The Gulf of Taranto (Southern Italy): seismic stratigraphy and shallow structure. Marine Geology 51, 327–346. http://dx.doi.org/10.1016/0025-3227(83)90110-X.

Rossignol-Strick, M., 1985. Mediterranean Quaternary sapropels, an immediate response of the African monsoon to variation of insolation. Palaeogeography, Palaeoclimatology, Palaeoecology 49, 237–263. http://dx.doi.org/10.1016/0031-0182(85)90056-2.

Rossignol-Strick, M., 1999. The Holocene climatic optimum and pollen records of sapropel 1 in the eastern Mediterranean, 9000–6000 BP. Quaternary Science Reviews 18, 515–530. http://dx.doi.org/10.1016/S0277-3791(98)00093-6.

Rothwell, R.G., Rack, F.R., 2006. New Techniques in Sediment Core Analysis: An Introduction. Geological Society. 267. Special Publications, London 1–29.

Ruff, M., Wacker, L., Gäggeler, H.W., Suter, M., Synal, H.A., Szidat, S., 2007. A gas ion source for radiocarbon measurements at 200 kV. Radiocarbon 49, 307–314.

Rutten, A., De Lange, G.J., Ziveri, P., Thomson, J., Van Sanvoort, P.J.M., Colley, S., Corselli, C., 2000. Recent terrestrial and carbonate fluxes in the pelagic eastern Mediterranean; a comparison between sediment trap and surface sediment. Palaeogeography, Palaeoclimatology, Palaeoecology 158, 197–213. http://dx.doi.org/10.1016/S0031-0182(00)00050-X.

Sangiorgi, F., Capotondi, L., Combourieu Nebout, N., Vigliotti, L., Brinkhuis, H., Giunta, S., Lotter, A.F., Morigi, C., Negri, A., Reichart, G.-J., 2003. Holocene seasonal sea-surface temperature variations in the southern Adriatic Sea inferred from a multiproxy approach. Journal of Quaternary Science 18, 723–732. http://dx.doi.org/10.1002/jqs.782.

Santvoort, P.J.M., Lange, G.J., Langereis, C.G., Dekkers, M.J., Paterne, M., 1997. Geochemical and paleomagnetic evidence for the occurrence of “missing” sapropels in eastern Mediterranean sediments. Paleoceanography 12 (6), 773–786. http://dx.doi.org/10.1029/97PA01351.

Savini, A., Corselli, C., 2010. High-resolution bathymetry and acoustic geophysical data from Santa Maria di Leuca Cold Water Coral province (Northern Ionian Sea—Apulian continental slope). Deep Sea Research Part II 57, 326–344. http://dx.doi.org/10.1016/j.dsr2.2009.08.014.

Schilman, B., Bar-Matthews, M., Almogi-Labin, A., Luz, B., 2001. Global climate instability reflected by Eastern Mediterranean marine records during the late Holocene. Palaeogeography, Palaeoclimatology, Palaeoecology 176, 157–176. http://dx.doi.org/10.1016/S0031-0182(01)00336-4.

Shuman, B., Plank, C., 2011. Orbital, ice sheet, and possible solar controls on Holocene moisture trends in the North Atlantic drainage basin. Geology 39, 151–154. http://dx.doi.org/10.1130/G31387.1.

Spagnoli, F., Bartholini, G., Dinelli, E., Giordano, P., 2008. Geochemistry and particle size of surface sediments of Gulf of Manfredonia (Southern Adriatic Sea). Estuarine, Coastal and Shelf Science 80 (1), 21–30. http://dx.doi.org/10.1016/j.ecss.2008.07.008.

Synal, H.-A., Stocker, M., Suter, M., 2007. MICADAS: a new compact radiocarbon AMS system. Nuclear Instruments and Methods in Physics Research B 259, 7–13.

Thomson, J., Croudace, I.W., Rothwell, R.G., 2006. A Geochemical Application of the ITRAX Scanner to a Sediment Core Containing Eastern Mediterranean Sapropel Units. Geological Society. 267. Special Publications, London 65–77.

Thomson, J., Crudeli, D., De Lange, G.J., Slomp, C.P., Erba, E., Corselli, C., Calvert, S.E., 2004. *Florisphaera profunda* and the origin and diagenesis of carbonate phases in eastern Mediterranean sapropel units. Paleoceanography 19. http://dx.doi.org/10.1029/2003PA000976 (PA3003).

Tjallingii, R., Röhl, U., Kölling, M., Bickert, T., 2007. Influence of the water content on X-ray fluorescence core-scanning measurements in soft marine sediments. Geochemistry, Geophysics, Geosystems 8. http://dx.doi.org/10.1029/2006GC001393 (Q02004).

Trigo, R., Xoplaki, E., Zorita, E., Luterbacher, J., Krichak, S.O., Alpert, P., Jacobeit, J., Sáenz, J., Fernández, J., González-Rouco, F., Garcia-Herrera, R., Rodo, X., Brunetti, M., Nanni, T., Maugeri, M., Türke, M., Gimeno, L., Ribera, P., Brunet, M., Trigo, I.F., Crepon, M., Mariotti, A., 2006. Chapter 3 relations between variability in the Mediterranean region and mid-latitude variability. In: Lionello, P., M.-R., P., Boscolo, R. (Eds.), Developments in Earth and Environmental Sciences. Elsevier, pp. 179–226.

Trouet, V., Esper, J., Graham, N.E., Baker, A., Scourse, J.D., Frank, D.C., 2009. Persistent positive north Atlantic oscillation mode dominated the medieval climate anomaly. Science 324, 78–80. http://dx.doi.org/10.1126/science.1166349.

Turchetto, M., Boldrin, A., Langone, L., Miserocchi, S., Tesi, T., Foglini, F., 2007. Particle transport in the Bari Canyon (southern Adriatic Sea). Marine Geology 246, 231–247. http://dx.doi.org/10.1016/j.margeo.2007.02.007.

Versteegh, G.J.M., de Leeuw, J.W., Taricco, C., Romero, A., 2007. Temperature and productivity influences on $U^{K'}_{37}$ and their possible relation to solar forcing of the Mediterranean winter. Geochemistry, Geophysics, Geosystems 8. http://dx.doi.org/10.1029/2006GC001543 (Q09005).

Vigliotti, L., Verosub, K.L., Cattaneo, A., Trincardi, F., Asioli, A., Piva, A., 2008. Palaeomagnetic and rock magnetic analysis of Holocene deposits from the Adriatic Sea: detecting and dating short-term fluctuations in sediment supply. The Holocene 18, 141–152. http://dx.doi.org/10.1177/0959683607085605.

Vilibić, I., Orlić, M., 2002. Adriatic water masses, their rates of formation and transport through the Otranto Strait. Deep-Sea Research II 49, 1321–1340. http://dx.doi.org/10.1016/S0967-0637(02)00028-6.

Von Breymann, M.T., Emeis, K.-C., Suess, E., 1992. Water Depth and Diagenetic Constraints on the Use of Barium as a Palaeoproductivity Indicator. Geological Society. 64. Special Publications, London 273–284.

Weltje, G.J., Tjallingii, R., 2008. Calibration of XRF core scanners for quantitative geochemical logging of sediment cores: theory and application. Earth and Planetary Science Letters 274, 423–438. http://dx.doi.org/10.1016/j.epsl.2008.07.054.

Weltje, G.J., Brommer, M.B., 2011. Sediment-budget modeling of multi-sourced basin fills: application to recent deposits of the western Adriatic mud wedge (Italy). Basin Research 23, 291–308. http://dx.doi.org/10.1111/j.1365-2117.2010.00484.x.

Yarincik, K.M., Murray, R.W., Peterson, L.C., 2000. Climatically Sensitive Eolian and Hemipelagic Deposition in the Cariaco Basin, Venezuela, Over the Past 578,000 Years: Results From Al/Ti and K/Al. Paleoceanography 15, 210–228.

Ziegler, M., Jilbert, T., Lange, G.J.d, Lourens, L.J., Reichart, G.J., 2008. Bromine counts from XRF scanning as an estimate of the marine organic carbon content of sediment cores. Geochemistry, Geophysics, Geosystems 9, Q05009. http://dx.doi.org/10.1029/2007GC001932.

Zonneveld, K.A.F., 1996. Palaeoclimatic reconstruction of the last deglaciation (18 ka. BP.–8 ka. BP.) In the Adriatic Sea region: a land–sea correlation based on palynological evidence. Palaeogeography, Palaeoclimatology, Palaeoecology 122, 89–106. http://dx.doi.org/10.1016/0031-0182(95)00091-7.

Zonneveld, K.A.F., Emeis, K.C., Holzwarth, U., Kniebel, N., Kuhnt, T., Möbius, J., Ní Fhlaithearta, S., Schmiedl, G., Versteegh, G., Welti, R., 2008. Report and Preliminary Results of *R/V POSEIDON* Cruise P339, Piräus–Messina, 16 June–2 July 2006. CAPPUCCINO—Calabrian and Adriatic Palaeoproductivity and Climatic Variability in the Last Two Millennia. Berichte aus dem Fachbereich Geowissenschaften der Universität Bremen. 268, pp. 1–61 (http://elib.suub.uni-bremen.de/ip/docs/00010656.pdf).

Zonneveld, K.A.F., Chen, L., Elshanawany, R., Fischer, H.W., Hoins, M., Ibrahim, M.I., Pittauerova, D., Versteegh, G.J.M., 2012. The use of dinoflagellate cysts to separate human-induced from natural variability in the trophic state of the Po River discharge plume over the last two centuries. Marine pollution bulletin 64, 114–132. http://dx.doi.org/10.1016/j.marpolbul.2011.10.012.